George Isaac

Ph.D. Thesis Title

ICE NUCLEI AND CONVECTIVE STORMS

ABSTRACT

Ph.D. Thesis Dept. of Meteorology

ICE NUCLEI AND CONVECTIVE STORMS

by

George A. Isaac

Surface atmospheric ice nucleus concentrations at -20C have been measured near Montreal, Quebec and Red Deer, Alberta. Frequency distributions of ice nucleus concentrations at these locations and at others in France, Australia and New Zealand, are log-normal with geometric standard deviations between 2.6 and 3.4. Concentrations of nuclei at -20C are approximately the same in both Alberta and Quebec; hour-to-hour variations can be greater than any slight difference in long term means of concentrations between the two provinces.

Large increases in ice nucleus concentration at -20C occur during precipitation (downdrafts) of Quebec and Alberta convective storms; there is no significant difference between hailing and non-hailing storms. If the observed higher ice nucleus concentrations in the storm downdraft mixed with a storm updraft of 10 m sec^{-1}, calculations indicate that no dramatic change would occur in the ice content of the updraft.

ICE NUCLEI AND CONVECTIVE STORMS

by

George A. Isaac, M.Sc.

A thesis submitted to the Faculty of Graduate Studies and Research of McGill University in partial fulfilment of the requirements for the degree of Doctor of Philosophy.

Department of Meteorology
McGill University

Montreal
April, 1972

ABSTRACT

ICE NUCLEI AND CONVECTIVE STORMS

Surface atmospheric ice nucleus concentrations at -20C have been measured near Montreal, Quebec and Red Deer, Alberta. Frequency distributions of ice nucleus concentrations at these locations and at others in France, Australia and New Zealand, are log-normal with geometric standard deviations between 2.6 and 3.4. Concentrations of nuclei at -20C are approximately the same in both Alberta and Quebec; hour-to-hour variations can be greater than any slight difference in long term means of concentrations between the two provinces.

Ice nuclei diffuse slowly toward cloud droplets. Cloud residence times in ice nucleus counters are very short; if most atmospheric ice nuclei activate by contacting or immersing themselves inside a water droplet, then ice nucleus counters may seriously underestimate the concentration of these nuclei. A comparison between laboratory and atmospheric clouds has been made with this particular problem being considered.

Large increases in ice nucleus concentration at -20C occur during the precipitation (downdrafts) of Quebec and Alberta convective storms; there is no significant difference between hailing and non-hailing storms. If the observed higher ice nucleus concentrations in the storm downdraft mixed with a storm updraft of 10 m sec^{-1}, calculations indicate that no dramatic change would occur in the ice content of the updraft.

PREFACE

Most of the data for this thesis was obtained in Alberta during the summers of 1969 and 1970, while the author participated in the field program of the Alberta Hail Studies (ALHAS) of the Research Council of Alberta. The excellent facilities provided by this organization have enabled ice nucleus concentrations near a storm to be compared with the radar structure, hail-fall pattern and surface wind and temperature fields created by the storm. The author is grateful for the assistance of the Alberta Hail Studies staff, especially Dr. P.W. Summers and Mr. R.H. Renick, in the preparation of the equipment and in the deployment of the mobile NCAR Ice Nucleus Counter. Each summer, two assistants helped with the ice nucleus counter measurements; the author is grateful to Mr. B. Wesley and Mr. D. Ristic for their contribution.

The patient counselling by Professor R.H. Douglas, who supervised the preparation of this thesis, was invaluable. Through private discussions and their own research, fellow-students Dr. B.L. Barge, Dr. C.W. Warner, Dr. A.J. Chisholm and Mr. I.I. Zawadzki aided in the presentation of storm radar data. Dr. Barge also helped in the collection and analysis of the hail data presented in section 4.3. Mr. Cheng-Wong Chang and Mr. Shue Fan Yip drafted the diagrams and Mr. P. Levert carried out all the photographic reductions. Mrs. E. Martin proof-read and typed most of the thesis.

The Atmospheric Environment Service, Environment Canada, the National Research Council of Canada, and the Research Council of Alberta provided financial assistance for the author.

The following points are original contributions to scientific knowledge about the atmosphere, which are a direct result of the Ph.D. research of the author.

(a) Frequency distributions of atmospheric ice nucleus concentrations, measured at temperatures between -15C and -21C over time intervals longer than two weeks, are log-normal with geometric standard deviations between 2.6 and 3.4. This was found to be true using four different techniques at four widely separated geographical locations and has been briefly described by Isaac and Douglas (1971). Many meteorological parameters are distributed log-normally; for example, it was found that frequency distributions of hailfall rates, hailstone dimensions and radar reflectivities of hail samples were log-normal.

(b) No evidence was found to suggest that ice nucleus concentrations in Alberta and in Quebec (at -20C) differ significantly either in absolute magnitude or in the scale of fluctuations.

(c) Large increases in ice nucleus concentrations at -21C are observed at the surface in the downdraft region of convective storms, both in Alberta and in Quebec. The magnitude of the concentration and the scale of fluctuations is the same for hailing and non-hailing storms.

(d) Cloud chambers might seriously underestimate the number of contact-freezing or immersion-freezing nuclei in the atmosphere. This particular problem has been mentioned before by Isaac (1968) and Sax and Goldsmith (1972), but a quantitative evaluation of the problem was first presented by Isaac and Douglas (1972).

(e) A new, more realistic, model of the transformation of cloud vapour and water into ice within a severe storm updraft has been developed. The ice content of a severe storm updraft is directly proportional to the ice nucleus concentration at a specific temperature. If the ice nucleus rich air observed in a convective storm downdraft mixed directly into the updraft air, the level at which a particular ice concentration was obtained would be lowered by approximately 0.75 km for a tenfold increase in nucleus concentration.

LIST OF FIGURES

LIST OF TABLES

TABLE OF CONTENTS

CHAPTER I

INTRODUCTION

Ever since Langmuir and Schaefer made their discoveries and hypotheses known about ice nuclei and cloud seeding potential, a tremendous amount of research has been directed towards identifying the sources and chemical composition and measuring the concentrations of naturally occurring ice nuclei. These studies have been difficult for three basic reasons. First, ice nuclei are small, probably less than 1 μm in diameter, and Vali (1966) suggests less than 0.01 μm. Second, Junge (1963) shows that a typical sample of inland air can contain 10^7 particles per litre but a typical concentration of ice nuclei at -20C might be one per litre (Mason, 1968). Not every particle is an efficient ice nucleus and consequently those particles which are must have some unique properties. Third, although it has been assumed for simplicity that ice nucleus concentrations are related only to supercooling, it now appears that cloud supersaturation (Gagin and Aroyo, 1969) and other parameters discussed in Chapter 5 are important.

Reviews of the literature on ice nuclei have been made by Bigg (1961), Soulage (1961), and more recently by Dufour (1966) and Mason (1968). There are three source regions for nuclei often mentioned: the surface of the earth, the stratosphere, and outer space. The surface of the earth is the most likely source, but the other two regions should not be ignored. Concentrations of ice nuclei at -20C are approximately the same throughout the world (Mason, 1968) from the poles to the equator. Bigg and Stevenson (1970) suggest that "the range of median concentrations around the world is smaller than the range of daily concentrations at one typical site". Fig. 1.1 shows the worldwide data

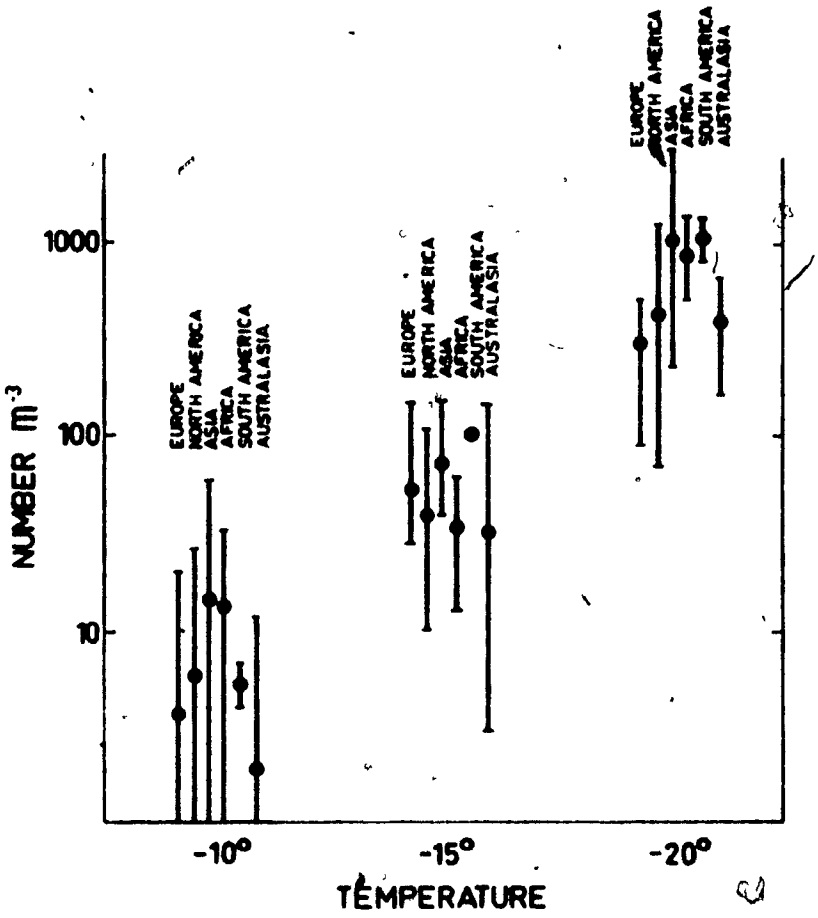

Fig. 1.1 Ice nucleus concentrations around the world. The range of median concentrations for each geographical group and the group mean are shown. (After Bigg and Stevenson, 1970)

of Bigg and Stevenson (1970). All the measurements were made using the Millipore filter technique (Section 2.2) and the filters were processed by the same method in two laboratories. This analytical procedure was very important, since wide variations in concentration can be obtained from different techniques and even from different observers using the same reported technique. Fig. 1.1 gives an idea of the ranges of concentration that can be expected, as well as the dependence of nucleus concentration upon temperature. Since worldwide variations are small, the theories of authors such as Bowen (1958) about extraterrestrial or non-tropospheric sources should not be completely ignored. However, there is little conclusive evidence to indicate either the chemical composition or the source region of atmospheric ice nuclei.

Soulage (1965) has remarked that current ice nucleus measurements should be labelled as the "pouvoir glacogene de l'air". That is, the number of ice nuclei activated is not necessarily equal to the resulting number of ice crystals. Ice crystals could fragment and splinters of ice might be created when drops freeze. Mossop (1970) has summarized some simultaneous comparisons of ice nucleus concentrations and ice crystal concentrations; the ratio of ice nuclei to ice crystals is usually much less than one, although Grant (1968) and Gagin (1971) have found ratios approximating one near -20C. This problem is considered in more detail in Chapter 5.

Many studies have attempted to relate ice nucleus concentrations to precipitation. Gagin (1965) found no relationship between ice nucleus counts at -15C and rainfall; however, by comparing precipitable water and an "effective" nucleus concentration, he was able to discriminate between rainy and dry weather. Georgii (1960) discovered that showers occurred on days with nucleus concentrations above average and continuous rain on days below average. When

rainfall increased from nil to 30 mm a day, Bigg and Miles (1964) found that the ice nucleus concentrations at -15C rose from approximately 175 to 450 nuclei per cubic meter. Isono and Tanaka (1966), Ryan and Scott (1969), and Rosinski et al. (1971) found maxima in ice nucleus concentration (at about -20C) during thunderstorms. During the passage of cold fronts, Buscaglione (1969) observed peaks in concentration which he was able to relate to instability. Isono et al. (1966) found a "close relation between the fallout rate of graupel pellets and snow crystals and the concentration of 'effective' ice nuclei which are active above cloud top temperatures". It is difficult to prove the hypothesis that natural ice nucleus concentrations influence precipitation. The positive results indicated above may only show that precipitation generates ice nuclei. This possibility will be discussed further in Chapter 6.

Will seeding cloud with ice nuclei affect precipitation? Two problems which are related to a future solution of this controversial question are discussed in Chapters 4 and 7. The probability that a certain seeding rate will exceed the background concentration of ice nuclei can be estimated from the data presented in Chapter 4. In Chapter 7, the possible effect of seeding severe storm updrafts is discussed using a hypothetical model storm. Little attention has been previously given to these specific problems. However, theoretical studies by Cotton (1970) and Jiusto (1971) suggest possible cloud seeding effects in small cumulus and layer clouds respectively.

CHAPTER II

ICE NUCLEUS COUNTERS

Ideally an ice nucleus counter should model the processes that lead to ice nucleation in natural atmospheric clouds. Consequently, the supersaturations and drop size distributions in cloud chambers should be carefully controlled as functions of temperature. Even if these parameters were known for all types of clouds, they would be difficult to reproduce; some approximations to actual cloud conditions must be made. Three different types of counters, which activate the nuclei in order to count them, are available. Cloud chambers which actually form clouds can be divided into two groups - mixing and expansion. Nuclei can be captured on supports such as filters or thermal precipitation slides and then activated and counted by cooling the support. Nuclei can also be detected in actual precipitation samples; this technique is restricted to periods where precipitation is occurring, but has the added advantage of activating nuclei which existed in clouds.

2.1 CLOUD CHAMBER TECHNIQUES

The necessary requirements for cloud chamber ice nucleus counters were outlined by Soulage (1965). Since activated nuclei can settle out of a cloud quickly, the resulting crystals cannot be counted by any method which assumes they remain suspended. The humidification process which produces the cloud must be carefully controlled. Since the walls in any chamber collect nuclei and water drops, a large volume-to-wall-area ratio is needed in order to minimize this problem. Because the nucleus concentration increases one order of magnitude for each 4C drop in temperature, rigid temperature control is required. All localized cold spots on the chamber walls must be eliminated

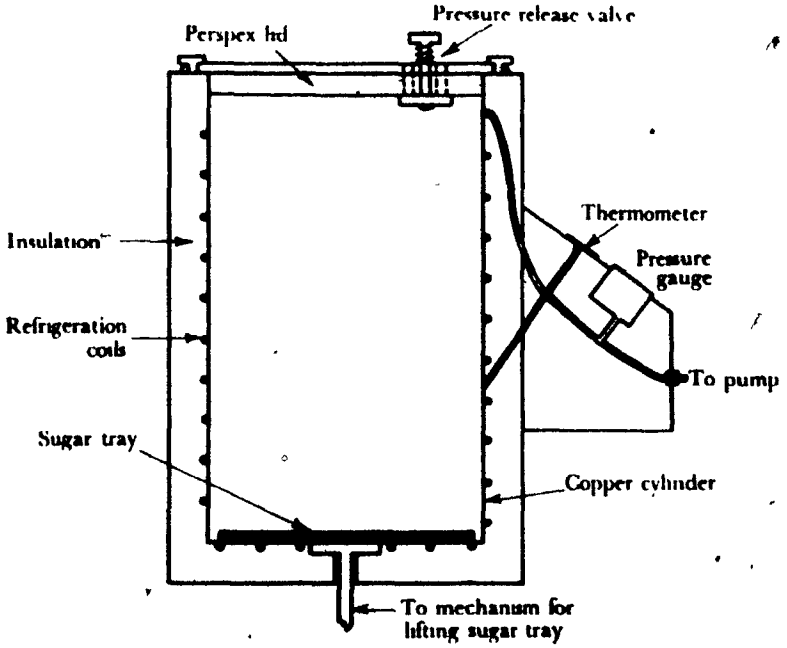

Fig. 2.1 The Bigg-Warner Ice Nucleus Counter. (After Fletcher, 1962)

or a representative operating temperature will be impossible to maintain, and the chamber walls must be kept ice free.

2.1.1 Mixing Chambers

The one-litre mixing chamber of Bigg (1957) was one of the earliest used. The inner walls were cooled by an encompassing cylinder containing a glycol/water mixture, and were kept frost free by careful wiping with glycerol. Air was replaced in the chamber mechanically. A cloud formed, together with a few ice crystals which then fell into a supercooled solution (usually sugar), and the crystals grew in this solution until they reached a visually countable size. Although this chamber was quite small, it was further enlarged and developed by Bigg and Meade (1959) and Hervier et al. (1967) into a continuously operated counter in which the air and solution were changed regularly. A photograph of the (sugar) solution provided the record.

A very simple mixing chamber method was described by Bigg (1965). A bubble of one- to five-litre capacity can be formed from a sugar solution with a little liquid detergent added. This bubble is placed into a cold box, and ice crystals form and fall onto the bubble wall and grow to a countable size. If performed correctly, this technique gives concentrations which agree with other mixing chamber methods.

2.1.2 Expansion Chambers

A widely used technique, described by Warner (1957) and Crozier (1969), cools the air by expansion. A 10-litre sample (Fig. 2.1) is cooled to -12C by conduction from the chamber walls, and then is cooled to the desired temperature by allowing the air inside to expand. The sugar solution of Bigg is used to count the crystals. In this chamber (hereinafter called the Bigg-Warner chamber) the operating temperature can be changed quickly by simply

changing the pressure to which the air is initially pumped into the chamber. However, the minimum temperature is achieved only for a few seconds since heat gradually seeps through the walls. Another practical difficulty often encountered involves contamination of the pressurization pump. AgI particles can quickly embed themselves inside the pump and cause spuriously high counts which can only be stopped by replacing this mechanism.

A large cloud chamber 6 feet in diameter and 9 feet high was constructed at Colorado State University (Steele and Smith, 1968) to simulate expansion or lifting of parcels of air under adiabatic conditions. Lapse rates of 0.5 to 5 C per minute within a temperature range of +20 to -50C and a pressure range of 200 to 1000 mb were possible. Heat transfer through the walls was eliminated by cooling. The large volume-to-wall-area ratio and the accurate temperature and pressure control made this chamber quite unique, but the ice crystal detection technique made the system unsuitable for measuring low atmospheric ice nucleus concentrations.

2.2 IMPACTION TECHNIQUES

Another type of ice nucleus counter captures the nuclei on a support along with all other atmospheric aerosols. In the thermal precipitator method designed by Fenn and Weickmann (1959), the particles were collected on the cool plate and then the plate was humidified and cooled; the number of droplets which froze at a predetermined temperature gave the concentration of ice nuclei. Using a Goetz Aerosol Spectrometer, a high-speed centrifuge, Gerber et al. (1970) size-sorted the aerosols and deposited them on a polished chrome foil. By cooling and supplying moisture, the foil was processed and the resulting number of crystals counted.

Bigg et al. (1963) described a method for measuring ice nucleus concentra-

tions by using Millipore filters. Air was drawn through a Millipore filter backed with a supporting disk. After exposure, the filters were processed by two different methods (Bigg and Stevenson, 1970) - a forced ventilation or a diffusion chamber technique. The Millipore technique is becoming very popular because of its reliability and the ability to inexpensively sample air at many remote stations while all the processing is done later at one laboratory.

2.3 THE DROP-FREEZING TECHNIQUE

Another technique described by Stansbury and Vali (1965) and Vali (1971a) measures the nucleus concentration within precipitation samples (snow, rain and hail). The collected sample is stored frozen until required. Then drops of the melted sample are put on a copper surface which has been covered with aluminum foil coated with an oil. The oil enables stable semi-hemispheric drops to form which do not alter shape during the cooling process, and it eliminates the possibility that any micro-scratches on the aluminum surface would act as nucleating sites. The copper surface is cooled and its temperature is recorded as each individual drop freezes. The freezing temperatures of a sample of N drops can be converted into an ice nucleus concentration by the following formula:

$$K(T) = -\frac{1}{V} \ln \frac{N(T)}{N(0)} \qquad (2.1)$$

$N(T)$ = number of unfrozen drops at temperature T (C)

$N(0)$ = total number of drops

$K(T)$ = number of nuclei per unit volume active at T or above

V = volume of individual drop

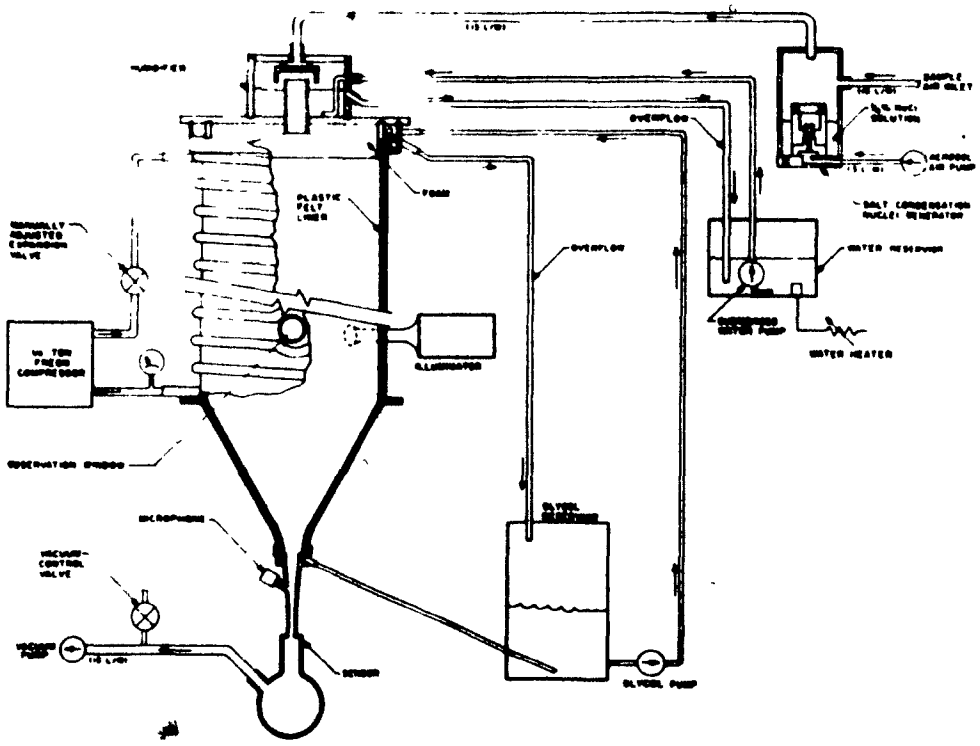

Fig. 3.1 The NCAR Acoustical Ice Nucleus Counter. (After Steele et al., 1967)

CHAPTER III

EQUIPMENT

3.1 CHARACTERISTICS OF THE NCAR ACOUSTICAL ICE NUCLEUS COUNTER

The preceding chapter has described some equipment which is generally used in measuring ice nucleus concentrations. The Bigg-Warner counter was used for some measurements to be described in section 4.1, and some precipitation samples described in Chapter 6 were analyzed by the method of Vali (1971a). Millipore filter technique measurements of Bigg and Miles (1964) and mixing chamber results of Hervier et al. (1967) have been re-analyzed for use in section 4.1. However, the instrument used for most of the data presented in Chapters 4 and 6 was the NCAR Acoustical Ice Nucleus Counter; a brief description of this instrument follows.

The NCAR Acoustical Ice Nucleus Counter (Langer et al., 1967) is basically a mixing chamber which uses a new technique for measuring the number of ice crystals within the chamber. The machine (Fig. 3.1) continuously draws in air, usually at 13 litres per minute, humidifies and cools the sample to a desired temperature in a 28 litre refrigerated chamber. A glycol/water mixture circulates gradually through the foam lining in the chamber and prevents frost formation on the walls. After approximately a two minute mean residence time, the supercooled cloud, including water droplets and ice crystals activated by ice nuclei, is drawn through a small capillary. When a particle greater than some threshold size passes through this capillary, an audible click results which is detected by a microphone and counted by a rate computer. The exact cause for this click is unknown, but a theoretical explanation is proposed by Dr. M. N. Plooster (Langer, 1966); when a particle

leaves the capillary, a sudden shift from laminar to turbulent flow causes a brief cessation of flow which results in the reflection of a shock wave up the capillary.

Since crystals grow to sizes greater than 40 μm diameter, while the water drops remain considerably smaller, the sensor is designed for a threshold of 40 μm. Langer (1966) has experimentally determined that when the sensor suction setting is from 3 to 7 inches of mercury, the generated signal amplitude is not a function of size for particles greater than 40 μm in diameter. The aerosol generator, by bubbling filtered air through a 0.25 percent salt solution, introduces condensation nuclei into the incoming air to insure the formation of a dense cloud with drops smaller than 10 μm. Because approximately 3 litres per minute of filtered air bubbles through this aerosol generator, the counter actually samples 10 litres of atmospheric air every minute.

An NCAR-Bollay Rate Computer, model 102, was used as the electronic counting system. This instrument totalizes the crystals counted and automatically displays a reading in counts per minute on the most appropriate of four scales. The four scales have maximum readings of 10^1, 10^2, 10^3 and 10^4 counts per minute, totalizing over 2 minutes, 12 seconds, 12 seconds and 1.2 seconds respectively. The first two scales overload after 20 crystals are counted while the next two can reach 200. The microphone in the sensor generates a sine wave pulse which, according to Steele et al. (1967), decays to 1/10th of its original value in 5 ms. To insure that a crystal is not counted more than once, the rate computer will not detect anything for a certain "dead time" (3 to 10 ms) after one is counted. To protect against false readings, 50 mv was taken as the threshold level on the incoming pulse.

Humidification was accomplished by passing the air over a heated water surface (near 40C) before introducing it into the chamber. Temperatures in the instrument were measured to within 0.25C with a thermocouple connected to a Varian recorder. Isaac (1968) has described the chamber temperature profile; the operating temperature specifies the temperature in the lower three quarters of the chamber.

Many criticisms have been made of this particular counter. These have been very general comments (Bigg, 1970a) which have been unverified experimentally. For example, it has been stated that the humidification system and aerosol generator create water drops large enough to trigger the sensor. The author can filter the incoming air with a Millipore filter and at -20C, the instrument will not detect more than one crystal per 1500 litres; this is far below background. Langer (1971) has replied to some of the criticisms and has agreed that the humidification system and aerosol generation system used in the equipment described above are unsuitable. Langer and Weickmann (1971) have outlined improvements which should be incorporated. However, even these suggested improvements have never been compared with unmodified equipment.

Bigg (1970b), Langer (1969) and Steele et al. (1967) have made comparisons of this machine with other equipment and their reports suggest correction factors which could be applied to NCAR Ice Nucleus Counter measurements. The correction factors would raise the NCAR Counter readings to a more "realistic" value. However, even these correction factors vary a great deal (3 to 15) and although Langer (1971) suggests the NCAR Counter reads low because some crystals hit the lower chamber walls without going through the sensor, the fractional percentage differs from report to report (Langer, 1971; Langer and Weickmann, 1971).

The lack of any absolute standard for ice nucleus measurements makes the NCAR Ice Nucleus Counter concentrations only qualitative. At the moment, the NCAR Counter is the only continuous recording instrument; although it has many deficiencies, it does detect whether concentrations are increasing or decreasing. Chapter 4 suggests that the magnitude of the fluctuations is identical to those of other equipment. In this thesis, the concentrations as given by the NCAR Counter are not considered as "real" concentrations of ice nuclei. Although comparison with other equipment shows that the instrument records about a factor of 3 to 5 low (Bigg, 1970b), this error is not considered a serious restriction to the conclusions presented.

Most of the measurements presented have been made with a chamber temperature of -20C. This temperature was chosen because each rate computer reading was rarely zero at this value. This meant that fluctuations in concentration could be detected within at least 2 minutes.

3.2 MEASUREMENT LOCATIONS AND AUXILIARY EQUIPMENT

Measurements were made at Macdonald College, Quebec and at various places in Alberta using the NCAR Acoustical Ice Nucleus Counter. The Quebec measurements described by Isaac (1968) have been extensively re-analyzed in this report. An attempt was made during the summers of 1969 and 1970 to measure variations of surface ice nucleus concentrations within and around Alberta hailstorms. Consequently, an NCAR Ice Nucleus Counter was mounted inside a van truck which was also equipped with a portable roof-mounted wind vane and anemometer mast, a rooftop rain/hail separator which funnelled the rain through a raingauge and allowed hail to be collected, and temperature and humidity gauges which were located inside the truck and were ventilated by a powerful fan. During 1969, the humidity gauge was a simple

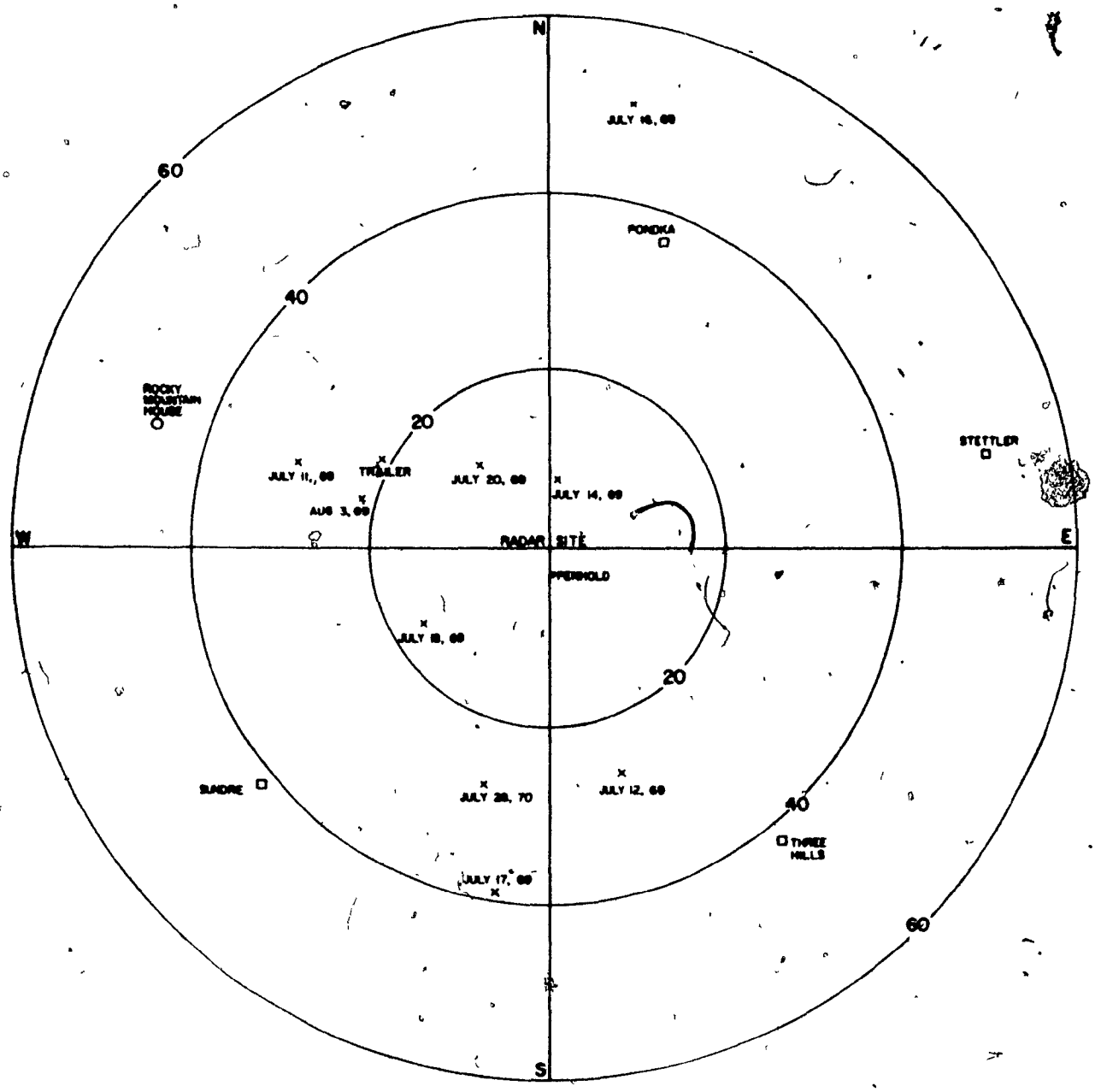

Fig. 3.2 A map of the locations where measurements were made in Alberta. Each site is labelled with the date the observations were taken. Range rings at 20 mi intervals from the radar are shown.

dial instrument accurate to within two percent. In 1970, this gauge was replaced by a more accurate wet-bulb thermometer which was identical to the standard dry-bulb thermometer ($\pm$0.1C). The temperature, humidity and wind instruments were read every minute. A fast recording raingauge was used which tipped every 0.17 mm of rain; the event was marked on a chart advancing at 90 inches per hour. The ALHAS radar (Barge, 1971) was used to direct the truck into the path of oncoming storms. Radio communications were maintained with the radar site (Fig. 3.2) and the truck at all times.

During 1970, a counter was operated in a trailer at Benalto (Fig. 3.2) in order to have another site available for measurements if a storm passed over it, and to determine the diurnal variations in ice nucleus concentration. However, the internal temperature of the trailer varied from 100F to 50F; this influenced the chamber temperature by as much as 3C, making the interpretation of these results uncertain. Consequently, these readings have not been included in this report. On one occasion, an early morning storm passed over the site; these readings are presented since the problem mentioned above was not critical for the short period presented. During storms observed from the truck, the chamber temperature was measured periodically and did not change significantly.

CHAPTER IV

FREQUENCY DISTRIBUTIONS OF ATMOSPHERIC ICE NUCLEUS CONCENTRATIONS

Frequency distributions of atmospheric ice nucleus concentrations, measured at some specified temperature, are strongly positively skewed. Consequently the arithmetic mean is not the best measure of central tendency, although it is the one most frequently used in the literature, both in quoting results of experimental measurements and in comparing measurements made at different locations and at different times. Frequency distributions of ice nucleus concentrations obtained with four types of counters, operated at several locations and at various temperatures, were found to be log-normal with geometric standard deviations between 2.6 and 3.4. Consequently, the geometric mean is a more meaningful parameter than the arithmetic mean.

4.1 THE LOG-NORMAL DISTRIBUTION

A log-normal distribution of X is defined by Irani and Callis (1963) as follows:

$$f(x) = \frac{1}{X\sqrt{2\pi}\ \ln \sigma}\ \exp\left\{-\left[\frac{\ln X/\bar{X}_G}{\sqrt{2}\ \ln \sigma}\right]^2\right\} \tag{4.1}$$

where $\bar{X}_G$ and σ are the geometric mean and geometric standard deviation as given by:

$$\log \bar{X}_G = \frac{1}{N}\sum_{i=1}^{N} \log X_i \tag{4.2}$$

$$(\log \sigma)^2 = \frac{1}{N}\sum_{i=1}^{N} (\log X_i - \log \bar{X}_G)^2 \tag{4.3}$$

The usual notation for a natural logarithm ($\ln$) and the logarithm to the base 10 (log) has been adopted. In a cumulative distribution of log X, the geometric

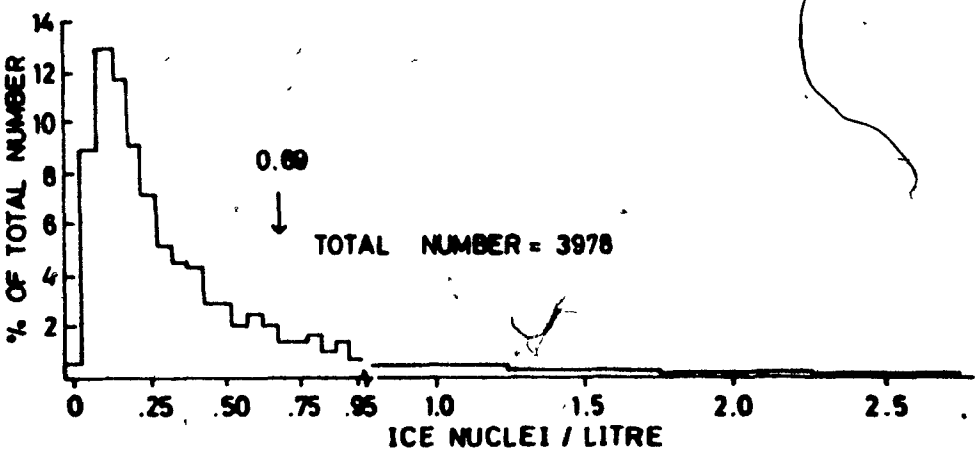

Fig. 4.1 Histogram of ice nucleus concentrations at -21C (150 litre samples) from 6 December 1967 to 26 January 1968. The break between .95 and 1.0 indicates a change in class interval. Percentages after .95 have been lowered by a factor of 10 to keep the area proportional to the percent of the total number.

standard deviation is the ratio of the 50 percentile value to the 16 percentile value, or the 84 percentile value to the 50 percentile value. If the cumulative distribution of X were plotted on log-probability paper, the "slope" of the resulting line is a direct measure of the geometric standard deviation.

Fig. 4.1 shows a histogram of nucleus concentrations at -21C measured with an NCAR Ice Nucleus Counter at Macdonald College, Quebec, from December 6, 1967 to January 26, 1968 (Isaac, 1968). A total of 3978 samples, each 150 litres in size, are used for the distribution. The arithmetic mean of 0.69 per litre is clearly not the best measure of central tendency of this skewed distribution. In Fig. 4.2, curve D shows the same data plotted on log-probability paper; with the exception of a slight irregularity near concentrations of 1 per litre (due to instrumental reasons), the points fall on a straight line. The distribution is log-normal and the best straight line fit (by eye) to the points gives a geometric mean of 0.26 per litre and a geometric standard deviation of 3.4; these compare favourably with the values calculated from the data, viz. 0.30 per litre and 3.2.

For a two-week interval during the sampling period mentioned above, a second NCAR Ice Nucleus Counter was operated at the same location under identical measuring conditions. Fig. 4.3 shows these simultaneous data (curves d_1 and d_2), together with curve D (reproduced from Fig. 4.2). During this comparison the geometric standard deviation for both counter distributions was 2.9 while the geometric means were 0.23 and 0.18 per litre (as determined from the graph). Besides showing that the data for these periods are both log-normal, Fig. 4.3 also indicates that the NCAR Ice Nucleus Counter produces consistent results; the concentrations are not dependent upon peculiarities, such as undetected wall cold spots, specific to one instrument.

CURVE	MEASURING TECHNIQUE	LOCATION	TEMP (C)	SAMPLE SIZE (l)	NO OF SAMPLES	GEOM. MEAN		GEOM. S.D.	
						GRAPH (l^{-1})	CALCULATED	GRAPH (l^{-1})	CALCULATED
A	MILLIPORE FILTER	AUSTRALIA NEW ZEALAND	-15	3×10^4		.067		3.2	
B	NCAR - BOLLAY	ALBERTA	-20	20	123	0.17	0.18	3.4	3.6
C	3005 - WARNER	ALBERTA	-21	10	123	0.10	0.23	2.6	2.4
D	NCAR - BOLLAY	QUEBEC	-21	150	3976	0.26	0.30	3.4	3.2
E	MIXING CHAMBER	FRANCE	-21	10	114	1.4		2.8	

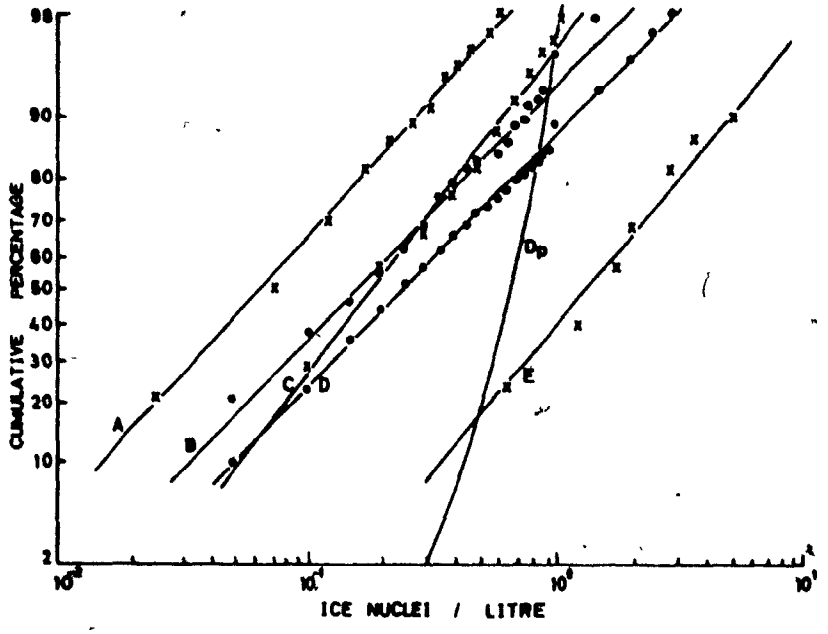

Fig. 4.2 Frequency distributions for measurements (A, B, C, D and E) mentioned in the above table. D_p refers to a hypothetical Poisson distribution calculated using the mean concentration of D.

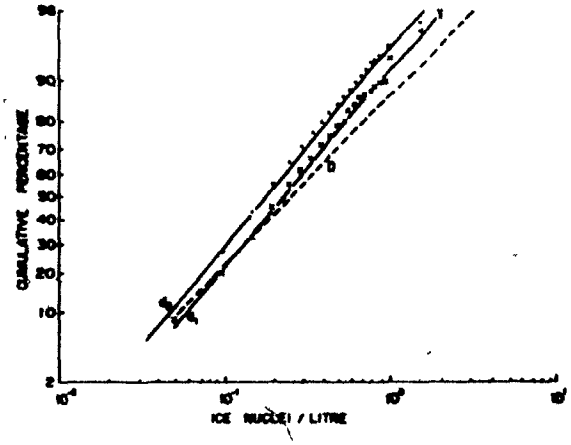

Fig. 4.3 A comparison of two NCAR Counters (d_1 and d_2).

Data from other sources have been added to Fig. 4.2 to provide additional evidence that such a distribution is of common occurrence. The measurement location, technique, temperature of operation and sample volume are listed in the table accompanying Fig. 4.2; the geometric standard deviations and the geometric means, determined from the best straight line fit and from calculations using the actual data (when available), are also tabulated. Curves B and C depict simultaneous measurements with an NCAR and a Bigg-Warner Ice Nucleus Counter at Penhold, Alberta over a two-week period in 1969; although there are only 123 samples for each curve, the distributions are similar. Curve A was deduced from the "no rain" data of the Millipore filter network of Bigg and Miles (1964); their data, compiled from an extensive network of 24 stations in Australia and New Zealand, are probably the best available. Curve E was deduced from the modified mixing chamber measurements of Hervier et al. (1967) in France. Regardless of location, method of measurement, sample volume, level of concentration and operating temperature, the distributions are all log-normal with geometric standard deviations between 2.6 and 3.4.

According to the Kolmogorov-Smirnov one-sample test (Siegel, 1956), the observed data of curves B, C and E of Fig. 4.2 and d_1 and d_2 of Fig. 4.3 can reasonably be thought to come from a population having the log-normal distribution indicated by their respective straight lines. At one nucleus per litre, the observed cumulative values of curve D of Fig. 4.2 have a maximum deviation from the fitted log-normal distribution which is significant at the probability level between .05 and .10 (two tailed test). However, the irregularity near one per litre shown on curve D was produced by the scale switching mechanism of the rate computer (see section 3.1). The data of curve D probably fit the

assumed log-normal distribution better than is indicated.

According to the Kolmogorov-Smirnov two-sample test (Siegel, 1956), curves B and C of Fig. 4.2 are drawn from a population with the same distribution. Curves d_1 and d_2 of Fig. 4.3 are different at the .001 significance level as indicated by the Kolmogorov-Smirnov two-sample test, perhaps because of a slight difference in operating temperature of less than 0.5C between the two ice nucleus counters.

While one would expect the geometric standard deviation to decrease with increasing sample volume, Fig. 4.2 indicates no such tendency. This may be explained on the basis of persistence; the autocorrelation coefficient of log-concentration for data D is 0.84. In the presence of an autocorrelation r, the standard deviation σ' of means of successive pairs of observations is:

$$\log \sigma' = \log \sigma[(1 + r)/2]^{\frac{1}{2}} \qquad (4.4)$$

(Munn, 1970)

where

$$r = \frac{1}{(N-1)(\log \sigma)^2} \sum_{i=1}^{N-1} (\log X_i - \log \bar{X}_G)(\log X_{i+1} - \log \bar{X}_G) \qquad (4.5)$$

Enlarging the sample volume of D from 150 to 1500 litres increases the geometric mean from 0.30 to 0.36 per litre and decreases the geometric standard deviation and autocorrelation coefficient from 3.2 to 2.8 and from 0.84 to 0.59 respectively. The geometric standard deviation will thus decrease very slowly with larger sample sizes. Because the geometric mean is dependent upon sample volume, this volume must be given when specifying the other distribution parameters.

4.2 THE POISSON DISTRIBUTION

According to Scrase (1935), if ice nuclei were distributed randomly in the atmosphere, a Poisson distribution of ice nucleus concentrations would be observed. For example, consider n nuclei in a total volume V which has been

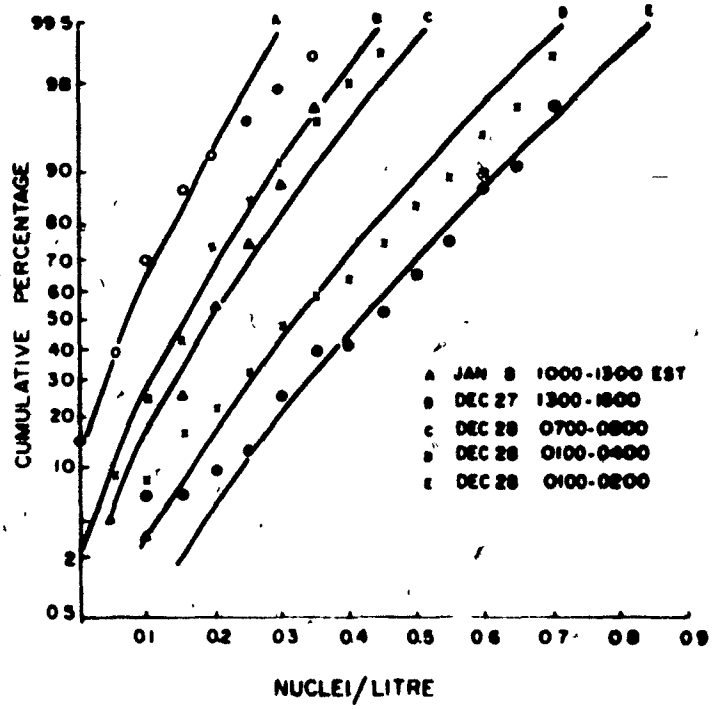

Fig. 4.4 Cumulative frequency distributions of ice nucleus concentrations for the indicated intervals. The solid lines represent Poisson distributions calculated using the arithmetic mean for each interval.

divided up into small samples v. The volume V consists of V/v samples, and the probability P_1 of restricting only one nucleus to a specific sample is:

$$P_1 = [(\frac{V}{v} - 1)^{n-1}/n - 1!]/[(\frac{V}{v})^n/n!]$$

$$P_1 = n\frac{v}{V}(1 - \frac{v}{V})^{n-1}$$

Similarly for two nuclei to a specific sample:

$$P_2 = \frac{n(n-1)}{2!}(\frac{v}{V})^2(1 - \frac{v}{V})^{n-2}$$

or, for x nuclei to a specific sample:

$$P_x = \frac{1}{x!}n(n-1) \ldots\ldots (n - x + 1)(\frac{v}{V})^x(1 - \frac{v}{V})^{n-x}$$

If $n \gg x$ and $v \ll V$

$$P_x = \frac{1}{x!}(\frac{nv}{V})^x e^{-nv/V}$$

Now the mean concentration m for sample v is nv/V. Thus

$$P_x = e^{-m} m^x/x! \qquad (4.6)$$

which is a Poisson distribution.

In Fig. 4.2, curve D_p is a Poisson distribution based on the arithmetic mean of the data of curve D. It is clear that the data of D, collected over a long period of time, are not well described by a Poisson distribution. This is not surprising; since sources and sinks of ice nuclei exist in the atmosphere, measurements made over long intervals such as a week would not be expected to fit a single Poisson distribution. When the data of curve D are broken into short periods (one to three hours in length), then the data from each such short period would be approximated by a Poisson curve, provided that the arithmetic means of adjacent periods are not increasing or decreasing. Illustrations of

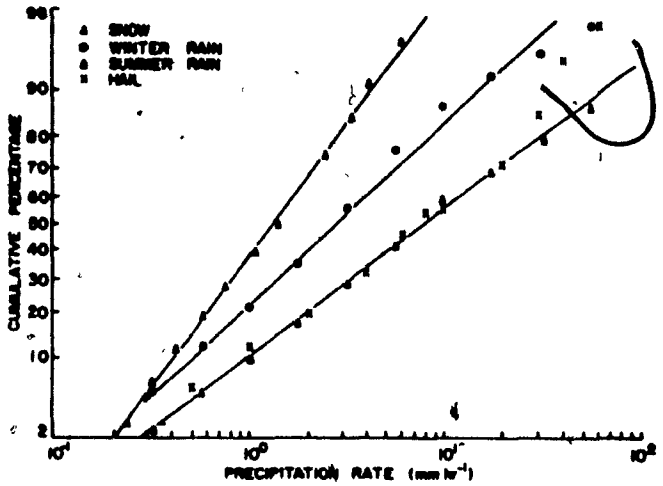

Fig. 4.5 Cumulative distributions of summer and winter rainfall, snowfall and hailfall rates.

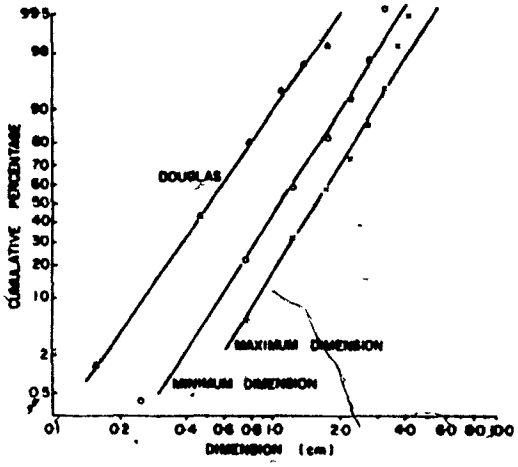

Fig. 4.6 Cumulative distributions of hail sizes. The distributions for maximum and minimum dimensions are shown for the data of Barge and Isaac (1970).

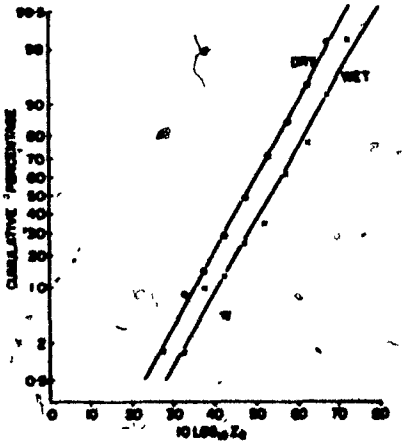

Fig. 4.7 Cumulative distributions of hail sample reflectivities assuming wet and dry hailstones and a 10 cm wavelength.

a few such periods are presented in Fig. 4.4, but these intervals do not occur often. The examples in Fig. 4.4 are constructed using 20 litre volumes as single samples. In 1 (3) hours, only 30 (90) samples can be used for the distributions.

4.3 OTHER METEOROLOGICAL EXAMPLES OF LOG-NORMAL DISTRIBUTIONS

Many frequency distributions of meteorological parameters can be approximated by log-normal curves. Fig. 4.5 shows the cumulative distributions of summer and winter rainfall, snowfall, and hailfall with rate plotted on log-probability paper. The Montreal rain curves have been obtained from Weiss (1964), the Montreal snowfall data from Gunn (1960), and the Alberta hailfall data from the 67 samples of Douglas (1963, 1965). Size distributions of particles are often log-normal (Irani and Callis, 1963), and the hail data of Barge and Isaac (1970) and Douglas (1965), as shown in Fig. 4.6, can be approximated by log-normal curves with the same geometric standard deviation. Fig. 4.7 shows that the reflectivities of hail samples (Douglas, 1965) can be approximated by log-normal curves. The calculated geometric means and geometric standard deviations of the hail data agree ~~with~~ those predicted from Figs. 4.6 and 4.7, but the raw precipitation rates for snow and rain of Fig. 4.5 are not available for such a check. The Kolmogorov-Smirnov one-sample test indicates that the hailfall rate, hail size, and hail reflectivity distributions of Douglas can reasonably be represented by their respective straight lines in Figs. 4.5, 4.6 and 4.7.

4.4 A PHYSICAL BASIS FOR THE LOG-NORMAL DISTRIBUTION

Munn (1970) attempted to explain why log-normal distributions are common and illustrates his discussion with an example from Zimmer and Larsen (1965). Aitchison and Brown (1957) discuss many non-meteorological examples of log-normal distributions and the physical basis of their generation. A brief

description of one of their lines of reasoning follows. If a series of numbers $(X_1, X_2, \ldots, X_j, \ldots)$ is obtained sequentially in time where X_2 follows X_1 and X_j follows X_{j-1}, the difference between any two of these numbers could be represented by

$$X_j - X_{j-1} = \epsilon_j X_{j-1} \tag{4.7}$$

where ϵ_j is a random and independent variable. The difference depends on the previous value of the variable. Now

$$\frac{X_j - X_{j-1}}{X_{j-1}} = \epsilon_j$$

$$\sum_{j=1}^{n} \frac{X_j - X_{j-1}}{X_{j-1}} = \sum_{j=1}^{n} \epsilon_j$$

and if the difference between X_j and X_{j-1} is small

$$\sum_{j=1}^{n} \frac{X_j - X_{j-1}}{X_{j-1}} = \int_{X_o}^{X_n} \frac{dX}{X} = \log X_n - \log X_o$$

$$\log X_n = \log X_o + \epsilon_1 + \epsilon_2 + \ldots + \epsilon_n \tag{4.8}$$

Using the additive form of the central limit theorem or the Lindeberg-Levy Theorem (Aitchison and Brown, 1969; Fisz, 1963), where $\log X_o$, ϵ_1, ϵ_2, ..., ϵ_n are independent and random variables which have the same distribution with a non-zero standard deviation, then $\log X_n$ has an asymptotically normal distribution.

The usual error analysis would show that

$$X_j - X_{j-1} = \epsilon_j \tag{4.9}$$

or

$$X_n = \epsilon_1 + \epsilon_2 + \ldots \epsilon_n + X_o \tag{4.10}$$

With the same conditions on X_o, ϵ_1, ϵ_2 ..., ϵ_n as above, X_n is asymptotically normally distributed.

The generation of the log-normal distribution, as it was described above, occurs because the variable follows the law of proportionate effect (Aitchison and Brown, 1957): "A variate subject to a process of change is said to obey the law of proportionate effect if the change in the variate at any step of the process is a random proportion of the previous value of the variate."

Intuitively many meteorological parameters would follow this law. For example, if the liquid water content or the updraft velocity of a storm increased or decreased, the corresponding change in the rainfall rate, from before to after the event, would not be random but would depend on the previous value of the rainfall rate. The analogy for ice nuclei is difficult to describe because of the lack of knowledge about variables affecting the activation of nuclei. However, ultraviolet radiation, relative humidity, wind speed and direction, and atmospheric stability are a few of the parameters often mentioned as influences on ice nucleus concentrations. Sources and sinks of ice nuclei also exist. If one parameter changed (for example, wind speed), the nucleus concentration would not be affected by a totally random amount as in Eq. (4.9) but would more likely follow Eq. (4.6).

4.5 SUMMARY

All ice nucleus measuring techniques appear to produce a log-normal distribution of concentrations with the same geometric standard deviation. If one gives an arithmetic mean, the distribution would not be adequately described; for example, 80 percent of the population of D (Fig. 4.2) is less than the arithmetic mean of 0.69 per litre.

Ice nucleus concentrations are not as erratic as some authors have des-

cribed. Although concentrations at the same temperature may not be comparable using different techniques, the magnitude of the fluctuations is similar, thus yielding a constant standard deviation.

A cloud seeder could use Fig. 4.2 to estimate how much his projected seeding concentration would exceed background. However, it must be cautioned that the data presented should not be considered as giving absolute concentrations.

CHAPTER V .

COAGULATION OF ICE NUCLEI WITH CLOUD DROPLETS

Many instruments used to determine ice nucleus concentrations count the number of ice crystals that form in an artifical cloud, and these results are frequently applied to natural clouds. This chapter examines the parameters affecting nucleation and how well the laboratory cloud simulates the natural one.

There are at least four different ways in which a particle may behave as an ice nucleus:

(a) Sublimation - direct deposition of water vapour on the particle.

(b) Condensation-freezing - a particle serves first as a condensation nucleus, then as a freezing nucleus.

(c) Contact-freezing - a particle initiates droplet freezing upon contact with the surface of the supercooled droplet.

(d) Immersion-freezing - a particle penetrates the droplet, then initiates freezing.

Each ice nucleus can probably activate by any one of the above methods, but it is unlikely that the nucleating temperature of the particle will be the same for each mode of activation. For modes (c) and (d), the particle must contact a droplet. The probability of such a collision in laboratory and natural clouds has been computed. Only a small fraction of aerosol particles ever collide with cloud droplets; the size of the aerosol particles, the cloud liquid water content, the droplet size distribution, and the time available for coagulation are important variables in this process. Some of these parameters are usually different in nature and the laboratory. If most nuclei prefer to activate through mode (c) and mode (d), then serious

errors may exist in a measured ice nucleus concentration if it is used for predicting the number of ice crystals occurring in a natural cloud.

5.1 COLLISION MECHANISMS

Aerosol particles collide with cloud droplets by means of several mechanisms; six are listed below.

1.) Brownian motion - Random motions of the particulates and cloud droplets cause collisions.

2.) Turbulent motion - Eddy diffusion around the droplets can cause collisions.

3.) Diffusiophoresis (Stefan flow) - Particulates move toward condensing droplets in the accompanying vapour pressure gradient.

4.) Langmuir collision - Falling droplets overtake and collide with particulates.

5.) Thermophoresis - Particles move toward evaporating drops in the accompanying temperature gradient.

6.) Electrical forces - Charged droplets and particulates might attract and thus collide with each other.

Slinn and Hales (1970) show that thermophoresis becomes important for below-cloud scavenging of particles 0.01 μm to 0.5 μm in radius when the temperature of the evaporating drops is 3C lower than that of the surrounding air and the rainfall rate is 10 mm hr^{-1}. Thermophoresis has been neglected in this chapter because a large temperature difference between the cloud air and its droplets is not likely. Both cloud droplets and aerosol particles are assumed to be electrically neutral; consequently, electrical forces are ignored.

The theoretical and experimental collision efficiencies of Davis and Sartor (1967), Woods and Mason (1964) and Hidy and Brock (1970) indicate

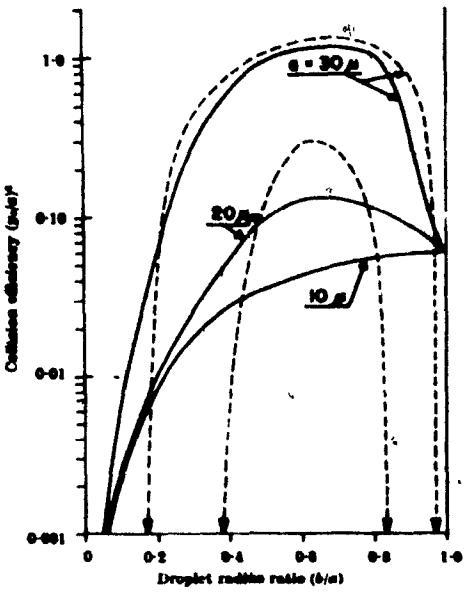

Fig. 5.1 Collision efficiency vs drop radius ratio. (After Davis and Sartor, 1967).

that capture by Langmuir collision can probably be neglected for particles less than 0.5 μm in radius. For example, in one second, cloud droplets of radius r, concentration N_c and terminal velocity c collect $\pi r^2 c N_c E(r_p)$ of the aerosol in the cloud, where $E(r_p)$ is the collision efficiency for aerosol particles of radius r_p. In a cloud of 1000 drops cm^{-3} of radius 10 μm, falling at 1 cm sec^{-1}, $E(r_p)$ is approximately 10^{-3} for aerosol particles 1 μm in radius (see Fig. 5.1) and so a fraction $10^{-6}\pi$ of the aerosol is collected in one second, or 10^{-2} in one hour. For smaller r_p, $E(r_p)$ and the fraction collected due to Langmuir collision is reduced.

In most cloud chambers used to count ice nuclei, the cloud-forming air is mixed with the ice nuclei and a fraction (E) of the aerosol is collected due to diffusiophoresis during cloud formation. Vittori and Prodi (1967) and Goldsmith et al. (1963) have discussed scavenging due to diffusiophoresis. A hydrodynamic flow of carrier gas exists toward (away from) a condensing (evaporating) surface, in the same direction as the diffusing vapour; airborne particles are thus carried toward a condensing surface. However, particles move in the direction of the diffusive flux of the heavier gas molecules in a binary gas mixture. For a condensing surface, the particles have a tendency to move away. Taking both mechanisms into consideration at S.T.P., the velocity (V_p) of the particles is given by

$$V_p = -1.9 \cdot 10^{-4} \frac{dP_1}{dx} \cdot$$

where the vapour pressure gradient is expressed in mb cm^{-1}. Ignoring the diffusive flux would result in an overestimate of V_p by approximately 20 percent, and the resulting simple formula would be

$$V_p = - \frac{D}{P_2} \frac{dP_1}{dx}$$

P_1, P_2 = partial pressures of vapour and gas (dynes cm^{-1})

D = diffusion coefficient of vapour in air.

Now

$$dP_1 = R_w T d\rho_1$$

where ρ_1 = density of vapour

R_w = gas constant for water vapour

T = temperature.

$$\frac{dm}{dt} = 4\pi r^2 D \frac{d\rho_1}{dr}$$

where r is the distance from the centre of the droplet. The velocity (v_p) of the particles toward the drop can be expressed as:

$$v_p = \frac{R_w DT}{P_2} \frac{d\rho_1}{dr} = \frac{R_w T}{P_2 4\pi r^2} \frac{dm}{dt}$$

The particle flux across the spherical shell is:

$$\frac{dN}{dt} = 4\pi r^2 n v_p = \frac{n R_w T}{P_2} \frac{dm}{dt}$$

where n is the particulate concentration and N is the number of particles captured. If one has a droplet concentration s, then

$$\frac{dn}{dt} = -s \frac{dN}{dt} = - \frac{s R_w n T}{P_2} \frac{dm}{dt}$$

$$n = n_o \exp(-s R_w Tm / P_2) \simeq n_o \left(1 - \frac{R_w Tw}{P_2}\right)$$

where n_o is the initial concentration and w is the liquid water content (gm gm^{-1}). The fraction (E) of particles collected can be expressed as:

$$E = \frac{n_o - n}{n_o} = \frac{R_w Tw}{P_2} \qquad (5.1)$$

For example, in the formation of a cloud at 950 mb and -20C with a liquid water content of 0.5 gm m^{-3}, the fraction of particles collected due to

diffusiophoresis is 6×10^{-4}.

Brownian and turbulent diffusion are the major mechanisms through which particles of radius less than 10,000 Å (1 μm) collide with cloud droplets. According to Greenfield (1957), if N_p and N_c represent the concentrations of aerosol (ice nuclei) and cloud drops respectively, then the rate at which aerosol particles are collected can be written as:

$$-\frac{dN_p}{dt} = (K_B + K_T)N_pN_c \qquad (5.2)$$

where:

$$K_B = \left(\frac{RT}{3kN}\right)\left(\frac{1}{R_p} + \frac{1}{R_c} + 0.9L\left(\frac{1}{R_p^2} + \frac{1}{R_c^2}\right)\right)(R_p + R_c)$$

$$K_T = \left(\frac{4v}{3}\right)(R_p + R_c)^3$$

$$L = (k\pi^{\frac{1}{2}})(2Pd_a)^{-\frac{1}{2}}$$

R = universal gas constant

t = coagulation time

P = pressure

k = coefficient of viscosity for air

L = mean free path of air molecules

N = Avogadro's number

v = gradient of air velocity across the streamlines

d_a = density of air

R_p, R_c = radius of nucleus, cloud drop

Brownian and turbulent motions are specified by the coagulation coefficients K_B and K_T respectively. Following Greenfield, the coagulation rate is maximized by using the large value of 30 sec^{-1} for v in the expression for K_T. The fraction (F) of particles captured by the cloud drops due to Brownian and turbulent diffusion, as a function of time, is given by:

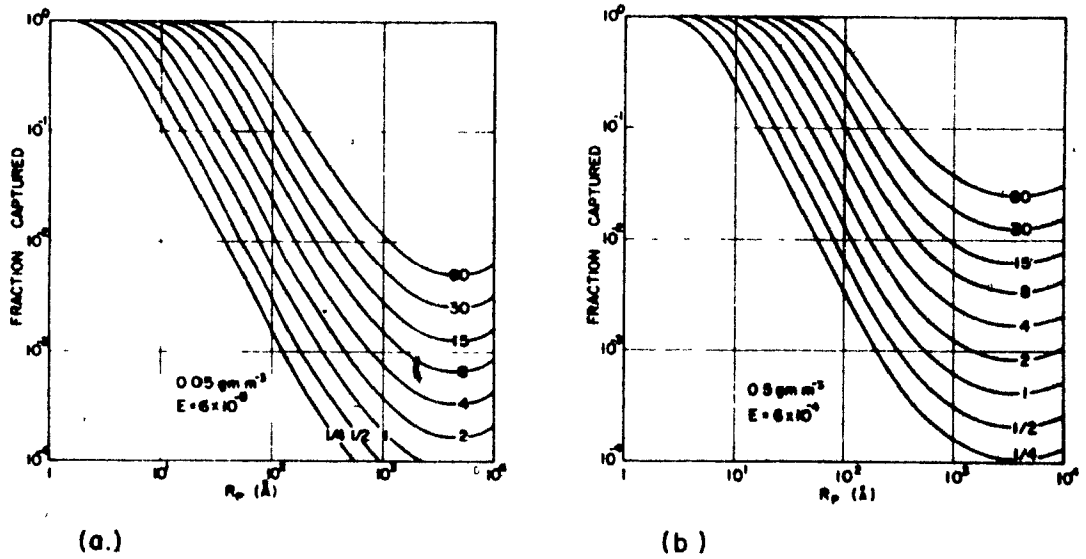

(a.) (b)

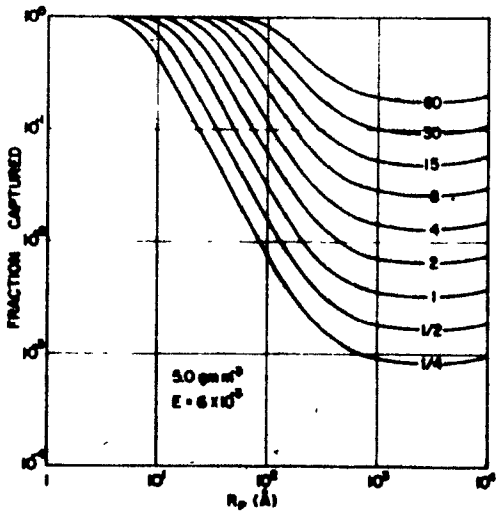

(c.)

Fig. 5.2 Fraction F of particles of a specific radius R_p that will be collected within the indicated time interval (minutes) due to Brownian and turbulent diffusion, in clouds with liquid water contents of 5.0, 0.5, 0.05 gm m^{-3} and 1000 droplets cm^{-3}. E indicates the fraction collected due to diffusiophoresis during cloud formation.

$$F = 1 - \exp(-(K_B + K_T)N_c t) \qquad (5.3)$$

This equation has been used to derive Figs. 5.2a, 5.2b and 5.2c, which show the fraction (F) of particles of a given radius that will be captured in a specified time by clouds of 0.05, 0.5 and 5.0 gm m^{-3} respectively, at -20C consisting of 10^3 drops cm^{-3} of radius 2.3 μm, 4.9 μm and 10.6 μm respectively. For example, 18 percent of particles of radius 100 Å will be collected in 15 minutes in the cloud of Fig. 5.2b. Although Eq. (5.3) has been solved for particle radii smaller than 50 Å, Junge (1963) has stated that the above theory is only well-founded for particles larger than this size. Calculations done for sizes much smaller than 50 Å can be regarded only as estimates.

Each time-curve in Figs. 5.2 reaches a minimum in the region of 10^3 to 10^4 Å where the fraction collected does not vary much with increasing particle radius. At this point K_T is becoming significant in Eq. (5.2); that is, turbulence is becoming the dominant mechanism for capture. Brownian diffusion provides nearlly all the transport at the smaller sizes. The minimum occurs near a particle radius of 0.4 μm in Fig. 5.2b, but this size would be increased to 0.8 μm if v were reduced from 30 sec^{-1} to 4 sec^{-1}, a value suggested by Whytlaw-Grey and Patterson (1932). The clouds of Figs. 5.2 already exist at time zero, but according to Eq. (5.1) a fraction (E) of the particles originally present was collected during cloud formation; this effect has not been considered in deriving Figs. 5.2.

Slinn (1971) has stated that Brownian diffusion is the dominant coagulation mechanism for particle radii between 10 Å to 10^3 Å. Alkezweeny (1971) states that Langmuir collision is the significant mechanism, but his collision efficiencies are dramatically different than those referenced

N_c (cm^{-3})			10^4			10^3			10^2		
w ($gm\ m^{-3}$)			5.0	0.5	0.05	5.0	0.5	0.05	5.0	0.5	0.05
P (mb)	t (min)	R_p (A)									
950	1	10	1.0	0.99	0.91	0.91	0.67	0.41	0.41	0.22	0.11
		10^2	0.13	0.060	0.028	0.031	0.013	0.0061	0.0089	0.0031	0.0013
		10^3	0.0064	0.0019	0.0008	0.0037	0.0006	0.0002	0.0031	0.0004	0.00006
		10^4	0.0053	0.0011	0.0004	0.0038	0.0005	0.0001	0.0033	0.0004	0.00005
950	15	10	1.0	1.0	1.0	1.0	1.0	1.0	1.0	0.97	0.81
		10^2	0.87	0.60	0.35	0.37	0.18	0.088	0.13	0.046	0.020
		10^3	0.091	0.029	0.013	0.053	0.0095	0.0029	0.045	0.0055	0.0010
		10^4	0.077	0.016	0.0059	0.056	0.0080	0.0016	0.048	0.0057	0.0008
450	1	10	1.0	1.0	0.99	0.99	0.90	0.66	0.66	0.40	0.21
		10^2	0.23	0.11	0.054	0.056	0.025	0.012	0.015	0.0057	0.0026
		10^3	0.0076	0.0025	0.0011	0.0039	0.0008	0.0003	0.0031	0.0004	0.00008
		10^4	0.0053	0.0011	0.0004	0.0038	0.0005	0.0001	0.0033	0.0004	0.00005
450	15	10	1.0	1.0	1.0	1.0	1.0	1.0	1.0	1.0	0.97
		10^2	0.98	0.83	0.56	0.58	0.32	0.16	0.20	0.083	0.038
		10^3	0.11	0.037	0.017	0.057	0.011	0.0038	0.046	0.0059	0.0011
		10^4	0.077	0.016	0.0060	0.056	0.0080	0.0016	0.048	0.0057	0.0008
Radius of drop (μm)			4.9	2.3	1.1	10.6	4.9	2.3	22.9	10.6	4.9

Table 5.1 Fraction (F, Eq. 5.3) of particles of radius R_p scavenged by a cloud of specified liquid water content (w), cloud droplet concentration (N_c) and pressure (P), in times of 1 and 15 min. v = 30 sec^{-1}, T = -20C.

above and since he quotes a formula by Slinn, it is unlikely this conclusion is valid. In the following, Langmuir collision has been neglected. A few estimates for the fraction collected by diffusiophoresis are included because this mechanism is important during the formation of a cloud and is probably the main cause for coagulation for particle radii between 10^3 and 10^4 Å in a cloud chamber with a short residence time, such as the Bigg-Warner instrument. Brownian and turbulent diffusion are considered the most important causes of nuclei-droplet coagulation.

5.2 COLLISION EFFICIENCY FOR ICE NUCLEI

According to Fletcher (1962), a spherical particle must have a radius of at least 10 Å in order to nucleate in one second whether by mode (b) or mode (d). Less than 70 percent of particles of this size enter the cloud droplets of Fig. 5.2b in one minute. Fletcher (1962) has also shown that a sublimation nucleus, mode (a), must be at least 100 Å in radius in order to activate in one second. Less than 2 percent of particles of this size enter the cloud of Fig. 5.2b in one minute. Consequently, particles which activate efficiently by mode (a) cannot be prevented from doing so by inadvertent introduction into water drops.

Table 5.1 summarizes the effect of some of the relevant parameters. The fraction (F) of particles captured is shown for four sizes of particles, two exposure times, and two pressures in nine different clouds at -20C. The calculations at 950 mb may be taken as representing a cloud chamber cloud, and at 450 mb an atmospheric cloud. Since most cloud chambers have residence times less than 15 minutes, computations have been made for 1 minute and 15 minutes. Diffusiophoresis has been neglected (since the value of E is 6×10^{-3}, 6×10^{-4} and 6×10^{-5} for clouds with liquid water

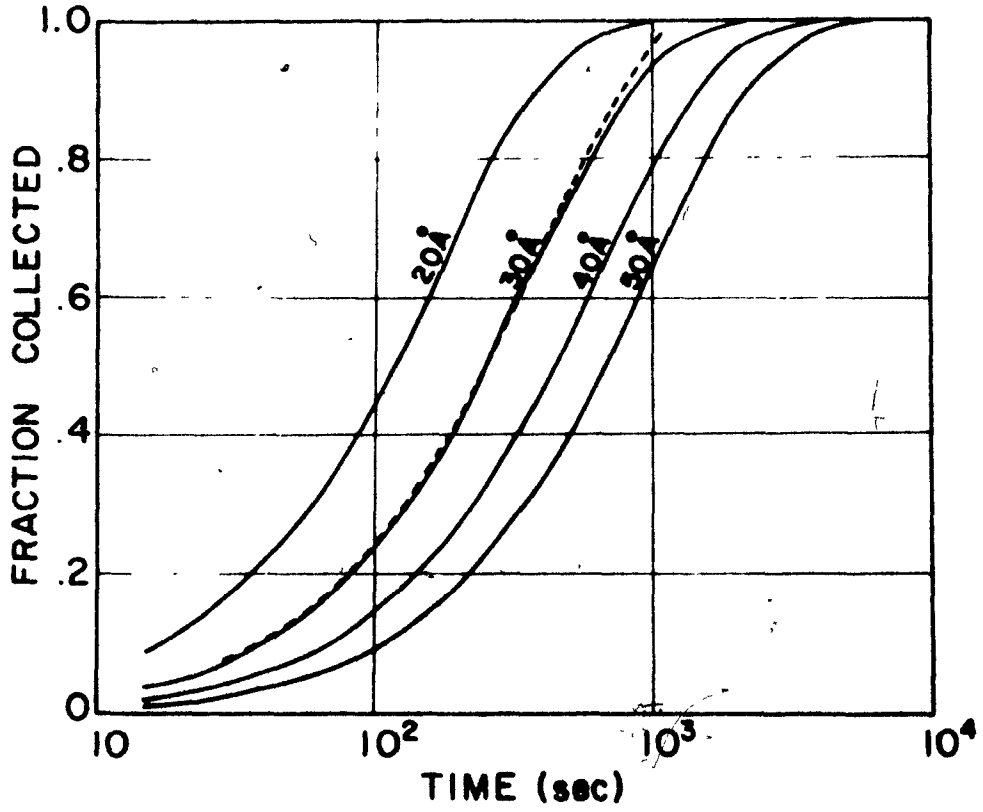

Fig. 5.3 The solution of Eq. (5.3) (solid lines) for various values of R_p using the cloud conditions of Warner and Newnham (1958), whose results (Eq. 5.4) are shown as the dashed line.

contents of 5.0, 0.5 and 0.05 gm m^{-3} respectively at 950 mb; at 450 mb, E increases by only a factor of 2).

Table 5.1 indicates that higher liquid water contents, lower pressures, and higher droplet concentrations make a cloud a more efficient scavenger. The differences in scavenging efficiency between two clouds are greatest for the largest particles. It is evident that an ice nucleus counter should maintain a constant droplet concentration as well as a constant liquid water content. The fraction of particles collected will also depend on the supersaturation within the cloud; a greater number of condensation nuclei are activated with increasing supersaturation, creating more cloud drops with approximately the same liquid water content.

5.3 EXPERIMENTAL OBSERVATIONS

Warner and Newnham (1958) found that the concentration of ice nuclei increased when their aerosol was allowed to co-exist with the cloud for periods as long as 20 minutes. They obtained the empirical relation

$$\frac{N_t}{N_{20}} = 1.04\left(1 - \exp\left(-\frac{t}{6.3}\right)\right) \qquad (5.4)$$

where N_t and N_{20} are the concentrations at time t and at 20 minutes. Using nucleation theory alone, Fletcher (1958) explained this effect by demonstrating that some nuclei required a considerable time to activate, but his numbers did not precisely fit Eq. (5.4). Fig. 5.3 is based upon Eq. (5.3) using the cloud conditions of Warner and Newnham (3000 drops cm^{-3}, 2.0 μm in radius). As Fig. 5.3 shows, the observations summarized by Eq. (5.4) could be explained by assuming that the nuclei were approximately 30 Å in radius and that they would not activate unless they collided with a droplet. The remarkable similarity between Eqs. (5.3) and (5.4) is

further evidence that coagulation of nuclei with cloud drops is a possible explanation of the above observations.

Steele and Davis (1969) found that the measured concentration of AgI ice nuclei at -12C increased by a factor of 1000 when the liquid water content of their cloud chamber changed from 0.8 to 2.5 gm m^{-3}. Although they tentatively suggested that the effect might be a "contact nucleation phenomenon", it cannot be completely explained on the basis of the mechanisms described in Table 5.1, unless the droplet concentrations in the two clouds were more than a factor 100 apart.

By heating a small amount of AgI in a test tube held in front of the NCAR Ice Nucleus Counter, it was found that the ice nucleus concentration at -16.5C could be varied from 0.2 to 400 $litre^{-1}$ by simply raising the humidifier temperature from 30C to 40C. This effect might be explained on the basis of a dramatic change in the liquid water content and the cloud drop concentration in the chamber. Visually, no appreciable change in these parameters took place but no instruments were available to confirm this observation. No dramatic dependence upon humidifier water temperature was detected with naturally occurring nuclei. Perhaps AgI is also directly sensitive to the value of supersaturation within the cloud. Gagin and Aroyo (1969) support this possible explanation in their Millipore filter technique observations.

5.4 CONCLUSIONS

As the pressure changes from 950 mb to 450 mb (Table 5.1), the fractions (F) for 10 Å and 100 Å increase by no more than a factor of 2, while those for 1000 Å and 10,000 Å change even less. Consequently, Figs. 5.2 (for 950 mb) can be consulted in considering the behaviour of a cloud at 450 mb.

If nucleation occurs by modes (c) and (d), then the effect of short (cloud chamber) versus long (natural cloud) residence times can be estimated from Figs. 5.2. In natural stable clouds where the residence time may be of the order of 60 minutes, at least 10 times more particles of radius 50 Å to 10,000 Å will be captured than in a laboratory cloud where times are usually under 2 minutes. Assuming a one-to-one correspondence between the number of ice crystals in a cloud and the number of ice nuclei that were initially present, one would observe more ice crystals at a specific temperature in a natural cloud than could be accounted for by an ice nucleus counter measurement at the same temperature.

Mossop (1970) has summarized measurements which show that ice nucleus concentrations can be much smaller than observed ice crystal concentrations. Hobbs (1969) and Auer et al. (1969) show that the ratio of ice crystals to ice nuclei decreases steadily from a value of 10^4 at -5C to about 1 at -25C. The calculations summarized in Table 5.1 could explain a portion of this departure from a one-to-one correspondence between measured nucleus concentrations and observed crystal concentrations. Since nuclei active at warmer temperatures are probably larger, and the fraction of aerosol collected by a cloud decreases with increasing particle size, the larger ratio at -5C (10^4) as compared with that at -25C (1) is logical.

Considering in addition the time lag effect of Fletcher (1958), little correlation can be expected to exist between ice nucleus concentrations and observed ice crystal concentrations, unless the mechanisms discussed above are taken into account. Takeda (1968) has shown that if nucleus measurements from laboratory clouds, existing for 1 minute, were applied to a large updraft of 14 m sec^{-1}, then the Fletcher time lag would not be serious. It is probable that the effect of a "coagulation" time delay

would also be reduced in large updrafts where the time spent between 0C and -40C is small (approximately 10 minutes in an updraft of 10 m sec^{-1}). Ice nuclei which could activate through modes (c) or (d) would not remain at any temperature level for very long, and would probably activate through modes (a) or (b) at lower temperatures. A cloud chamber successfully models these conditions.

For example, suppose that at a specific temperature there are 10 AgI contact nuclei, mode (c) or (d), to every AgI sublimation or condensation-freezing nucleus. These nuclei are introduced into an updraft of 10 m sec^{-1} at a cloud base of +5C; the cloud droplet concentration is assumed to be 1000 drops cm^{-3}. AgI nuclei tend to have a modal size between 10^2 Å and 10^3 Å (Gerber et al., 1970). During 6 minutes in a cloud of 0.5 gm m^{-3}, 3×10^{-3} and 6.5×10^{-2} of the 10^3 Å and 10^2 Å radius nuclei respectively are collected. Similarly, in a cloud of 5 gm m^{-3}, 1.8×10^{-2} of the 10^3 Å and 1.4×10^{-1} of the 10^2 Å nuclei are collected in 6 minutes. In these 6 minutes, the air parcel would reach the -15C level and although contact nuclei are 10 times more numerous than other nuclei, fewer than 10 percent of them are collected. Sublimation or condensation-freezing would then be the main activation mechanism. If however, the ratio of contact to non-contact nuclei is greater than 10, then contact nucleation would be the dominant mechanism.

No quantitative experiments have been conducted to determine accurately this ratio. Sax and Goldsmith (1972) and Slinn (1971) have discussed in a theoretical manner the nuclei-droplet coagulation problem as it relates to the number of AgI nuclei activated in an atmospheric cloud. Sax and Goldsmith (1972) have also mentioned that cloud chambers might underestimate

the number of atmospheric ice nuclei, but they do not discuss the problem quantitatively.

In analyzing precipitation samples by freezing drops, care should be exercised in applying the concentrations obtained to a severe storm updraft. For example, more nuclei are collected after an updraft parcel has risen above the -15C height level than before. If a -5C nucleus is detected, there is no guarantee that this nucleus was collected and activated at this temperature.

If the liquid water content or drop concentration varies in a cloud chamber, then the readings of the counter will vary if the nucleus concentration does not; spurious fluctuations can be introduced unless the cloud is controlled carefully. For example, if the liquid water content remains stable, but the cloud drop concentration changes by a factor of 10, Table 5.1 indicates that the "observed" concentration of ice nuclei could vary by a factor of 4.

AgI is a very effective contact-freezing nucleus but is relatively inefficient as an immersion-freezing nucleus (e.g. Guenadiev, 1970). If AgI is to be used effectively for cloud seeding, it must nucleate droplets by contact at a specific temperature and this process must not be pre-empted by the prior immersion of the particle within the cloud drop at a warmer temperature. This requirement poses many practical delivery problems.

Laboratory experiments should be conducted to determine the relative fraction of atmospheric ice nuclei which activate by the various modes. If the percentage which requires contact with cloud drops is small, then the time lag described in the above can be neglected.

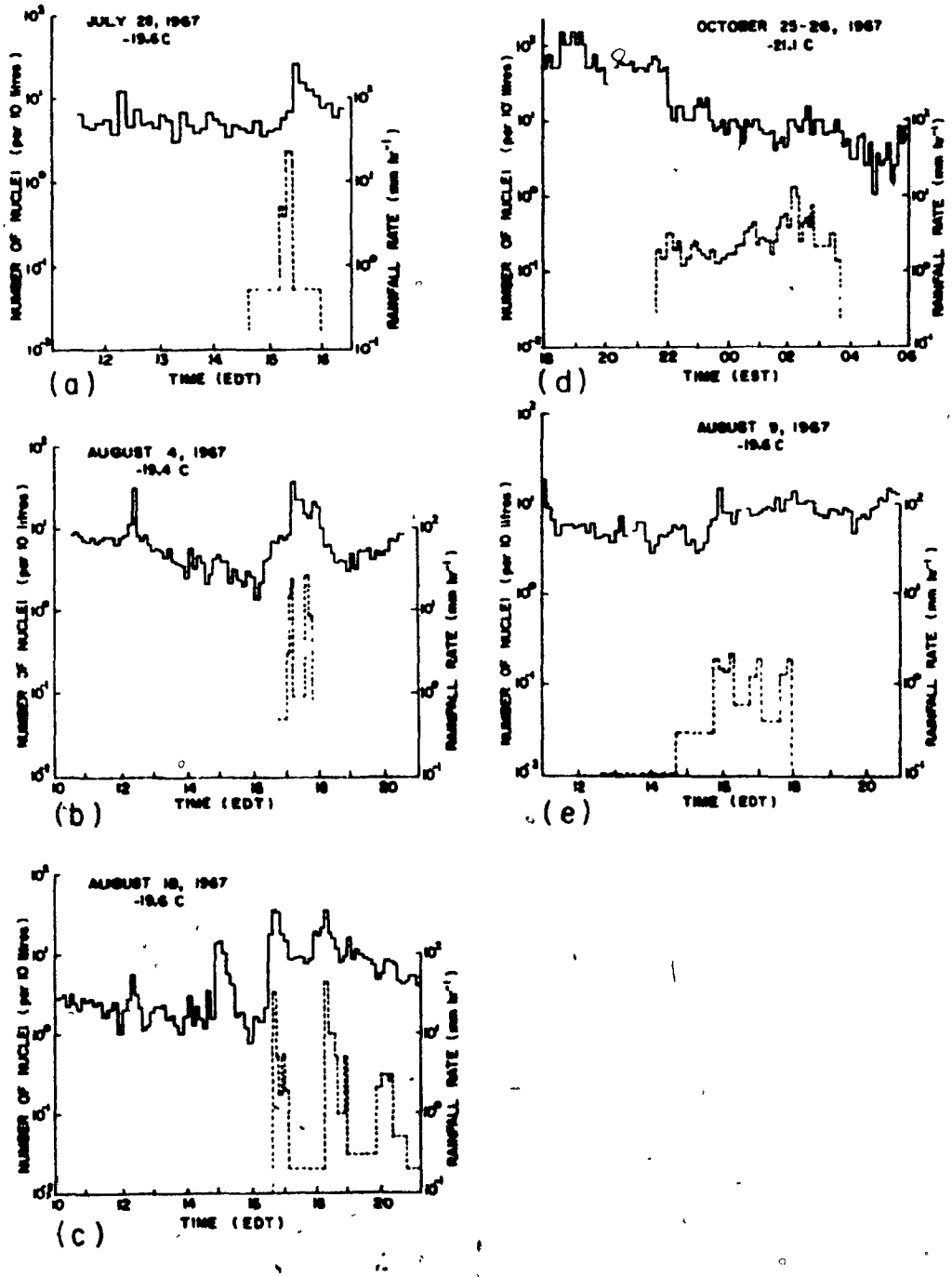

Fig. 6.1 Ice nucleus concentrations (solid lines) at the indicated temperatures and rainfall rates measured in Quebec. Cases a, b, and c represent convective rain; d and e represent continuous rain.

CHAPTER VI

ICE NUCLEUS CONCENTRATIONS BEFORE, DURING AND AFTER RAINFALL

The questions of whether ice nucleus concentrations affect precipitation and whether precipitation modifies ice nucleus concentrations were introduced in Chapter 1. This chapter examines and illustrates these questions using surface measurements of ice nucleus concentrations made before, during and after rainfalls in Quebec and Alberta. The equipment used has been described in Chapters 2 and 3.

6.1 ICE NUCLEUS CONCENTRATIONS AND QUEBEC RAINFALL

Fig. 6.1 shows the ice nucleus concentrations near -20C and the rainfall rate during 3 convective storms and 2 continuous storms that passed over Macdonald College, Quebec in 1967 (Isaac, 1968). The continuous storms are so labelled because the rainfall rate remains steady over a long period of time. In the storms labelled "convective", sharp and brief peaks in rainfall rate are observed.

The three thunderstorm (convective) rain cases of Fig. 6.1 all occurred in association with eastward-moving cold fronts oriented in a northeast to southwest line. The most dramatic features of these storms are the sharp peaks in ice nucleus concentration which occur almost simultaneously with the rainfall rate maxima. In Fig. 6.1a the ice nucleus concentration peak lags behind the rainfall rate peak, but in Figs. 6.1b and 6.1c the peaks occur simultaneously. Dust or dirt stirred up from the ground might explain the nucleus concentration peak of Fig. 6.1b and that associated with the first shower at 1630 EDT of Fig. 6.1c. However, during subsequent nucleus concentration peaks of Fig. 6.1c and that of Fig. 6.1a, the surface was wet before the ice nucleus concentration maximum occurred; ground dust would not have been stirred up easily.

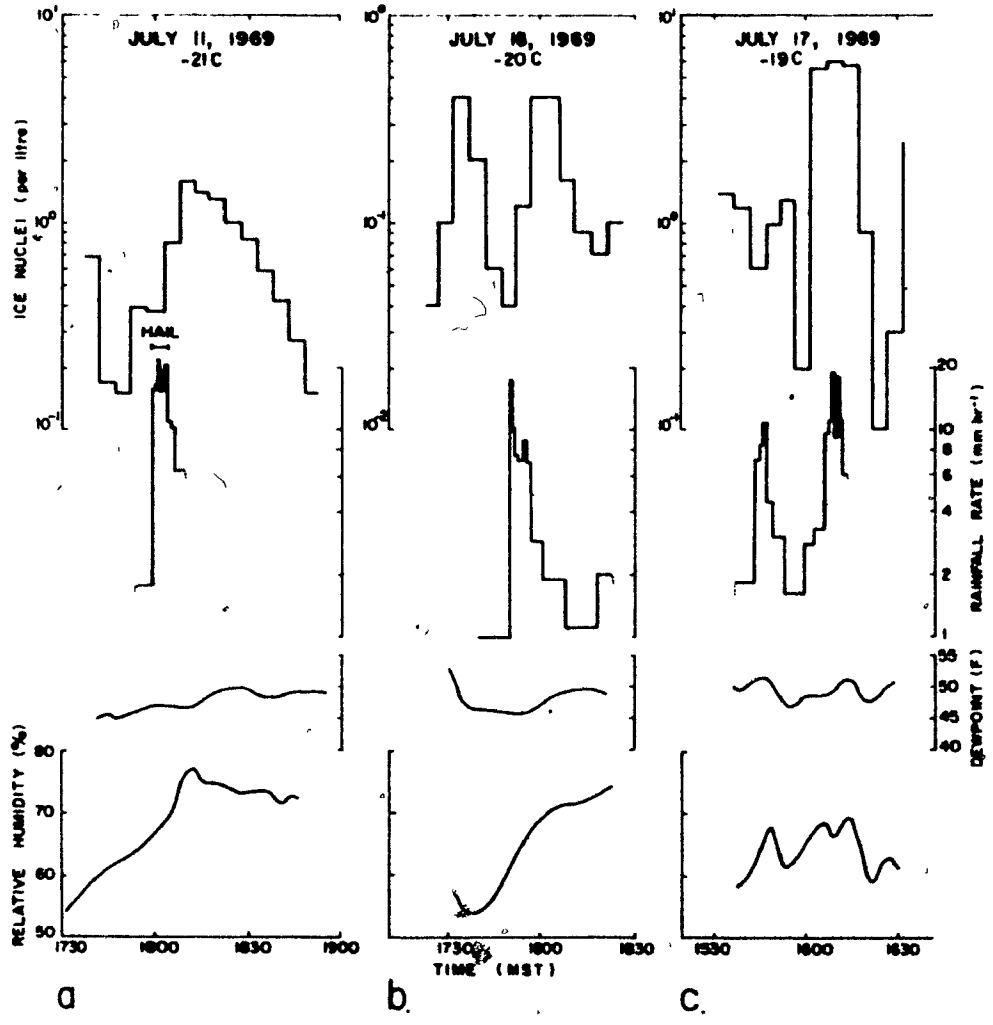

Fig. 6.2 Ice nucleus concentration, rainfall rate, dewpoint and relative humidity measured in Alberta on three days with thunderstorms.

Figs. 6.1d and 6.1e represent continuous rain cases. Perhaps because the rainfall rates were lower in Fig. 6.1e, the nucleus concentration increases slightly with the onset of rainfall, in comparison with Figs. 6.1a, b and c. During the continuous rainfall of Fig. 6.1d, the concentration decreases with the onset of rainfall! The decrease of Fig. 6.1d near 2200 EST can probably be attributed to a wind shift from 140° at 2100 EST to 210° at 2200 EST. This may mean a change in "air mass" was detected, or the air coming from different directions contains locally-produced but dissimilar aerosols. No dramatic, persistent wind shift occurred near the nucleus concentration peaks of Fig. 6.1 mentioned above. Hail was not observed during the thunderstorms of Fig. 6.1.

6.2 ICE NUCLEUS CONCENTRATIONS AND ALBERTA STORMS

Fig. 6.2 shows examples of the ice nucleus variations near three Alberta storms. A mobile NCAR Ice Nucleus Counter mounted in a truck and directed by the radar provided the readings. Rainfall rates, dewpoint temperatures and relative humidity have been plotted along with the ice nucleus readings. In contrast to Fig. 6.1, the measurements of Fig. 6.2 have been made over a much shorter time interval. The equipment had barely enough time to take a few readings before fluctuations took place. If during the storms of Fig. 6.2 a gust front occurred at the location, it is unlikely that the beginning was detected. Because of the shortcomings of Fig. 6.2, it was decided that the record should be lengthened, and the truck was directed to a site 30 minutes before the rainfall began.

The radar was an invaluable tool for describing some pertinent features of the storms wherein measurements were conducted. For example, on 11 July 1969 (Fig. 6.2a) the most intense portion of this small storm passed almost directly overhead, but the storm was weakening at that particular time. On 17 July 1969 (Fig. 6.2c) the most intense portion of the storm passed 4 mi south of the sampling location. The sharp drop in ice nucleus concentrations during the high rainfall rate of 16 July 1969 (Fig. 6.2b) may have been created because two

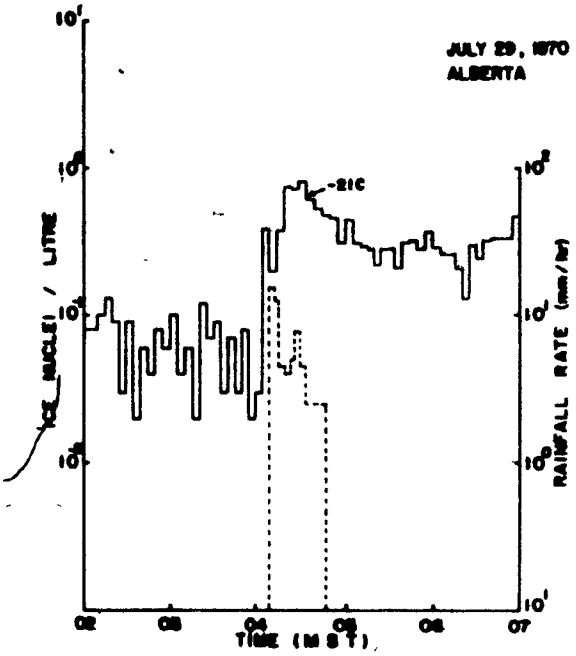

Fig. 6.3 Observations before, during and after an Alberta convective storm.

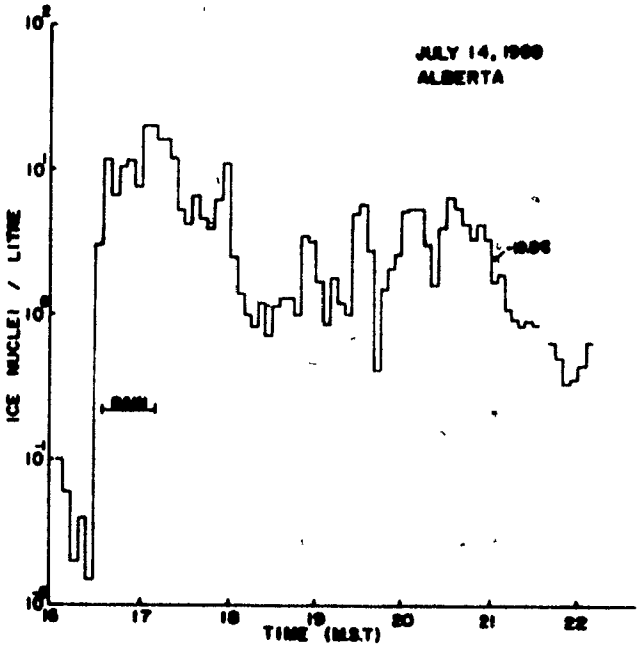

Fig. 6.4 Observations before, during and after an Alberta seeded storm.

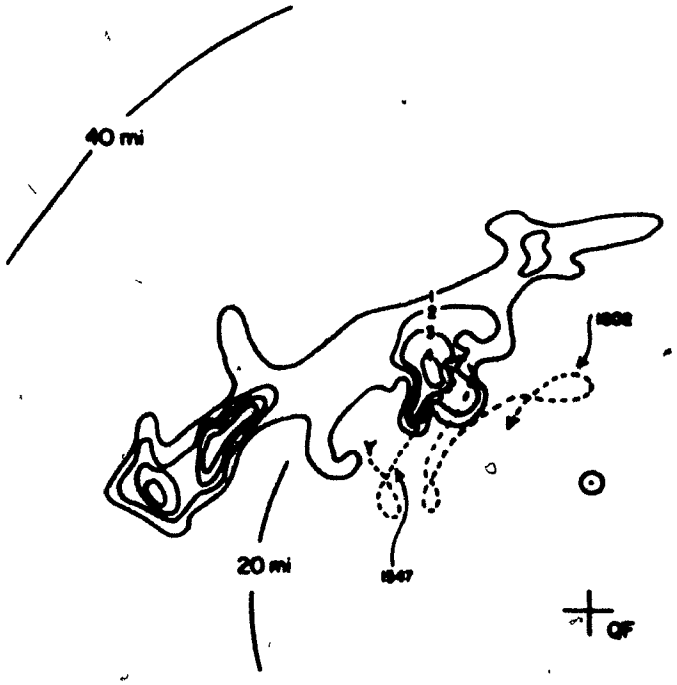

Fig. 6.5 Radar echo at 1603 MST 14 July 1969 (Fig. 6.4). Ze differs by a factor of 10 between each contour. The circle marks the sampling location for Fig. 6.4. The dashed line refers to the flight path of the seeding aircraft.

storms were passing, one on each side of the observing location, at approximately 1740 MST.

Fig. 6.3 shows the variations in ice nucleus concentrations during a thunderstorm that passed over the NCAR Counter installed in a trailer at Benalto. During this early morning storm, there was a lag of about 15 minutes between the onset of rain and the peaking of the nucleus concentration; a similar lag is seen in Figs. 6.1a and 6.2a. Consequently, it is probable that high rainfall rates do not directly produce large concentrations of ice nuclei through an evaporation mechanism as mentioned by Ryan and Scott (1969).

Fig. 6.4 shows an interesting case of the variations during a seeded Alberta storm. The storm was seeded from 1547 to 1602 MST with AgI flares fixed to a B-26 flying the updraft area at 6000 ft above ground. Fig. 6.5 shows the radar echo contours at $3/4^{o}$ elevation at 1603 MST, and the flight path of the aircraft. The rainfall rate at the sampling location (marked on Fig. 6.5) was less than 0.5 mm hr^{-1} since the main core of the seeded cell moved to the SW of the 1603 MST position.

A diagram with extended scales similar to Fig. 4.2, with curve B extrapolated, would indicate that concentrations of 20 per litre at -21C would be observed less than .01 percent of the time. Since nucleus concentrations of 20 per litre were observed on 14 July 1969 (Fig. 6.4) and the concentration jumped by a factor 1000 with the onset of rainfall, it is probable that AgI nuclei were detected. High ice nucleus concentrations aloft were brought to the ground during the storm. The ice nucleus concentrations remained at a high level for over 4 hours because the winds were very light after the storm had passed.

As Fig. 6.9 shows, rain samples (sample B being typical) from this storm were relatively "dirty". One cannot say that AgI was present in sample B, although such a presence would be expected on the basis of the cloud chamber readings shown in Fig. 6.4.

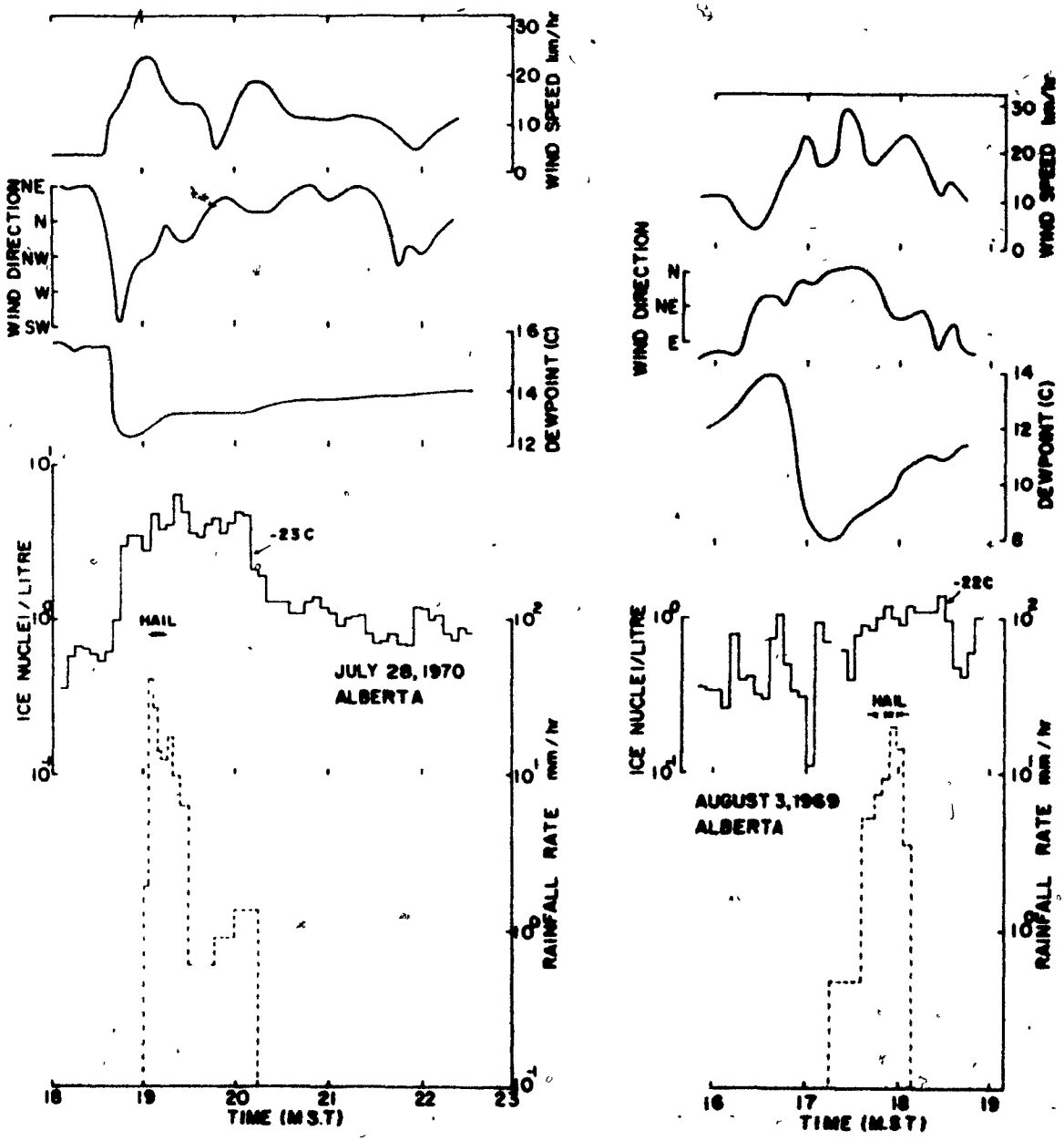

Fig. 6.6 Observations before, during and after two Alberta hailstorms.

6.3 A DETAILED STUDY OF TWO ALBERTA HAILSTORMS

Data were obtained during two Alberta storms when there was a long period (60 min) of measurements before the rain commenced and simultaneous measurements of surface wind, dewpoint temperature, and rainfall rate were available (Figs. 6.6a and 6.6b). Small shot- to pea-size hail fell during the indicated times at the observation sites, but walnut-size hail was observed in more intense portions of the storms.

The arrival of downdraft air associated with the gust front is easily recognized at about 1645 MST on 3 August (Fig. 6.6b) and at about 1840 MST on 28 July (Fig. 6.6a) by the dramatic drop in dewpoint, the wind shift and the increase in wind speed. These three parameters - wind speed, wind direction and dewpoint temperature - all reacted in a manner observed frequently by Byers and Braham (1949) during gust fronts. On 28 July, the concentration of ice nuclei increased simultaneously with the gust front; a similar, though less evident increase occurred on 3 August.

Fig. 6.7 and Fig. 6.8 show the radar echoes for these two storms displayed in HARPI* format (Zawadzki and Ballantyne, 1970) at 1900 MST for 28 July 1970 and at 1751 MST for 3 August 1969. In these figures, each section or panel shows the echoes in an annular ring, 3.2 km deep (i.e. in range), centered on the radar range indicated; coordinates are azimuth from the radar and height above ground. The sections are so arranged that one can imagine them as profiles of the storm at different distances from an observer, increasing from the bottom upwards. Fig. 6.8 was prepared electronically, and Fig. 6.7 by hand-construction, from the appropriate PPI scans. In both diagrams the location of the mobile truck, where the observations of Fig. 6.6a and Fig. 6.6b were made,

---

* HARPI: Height-azimuth-range-position-indicator

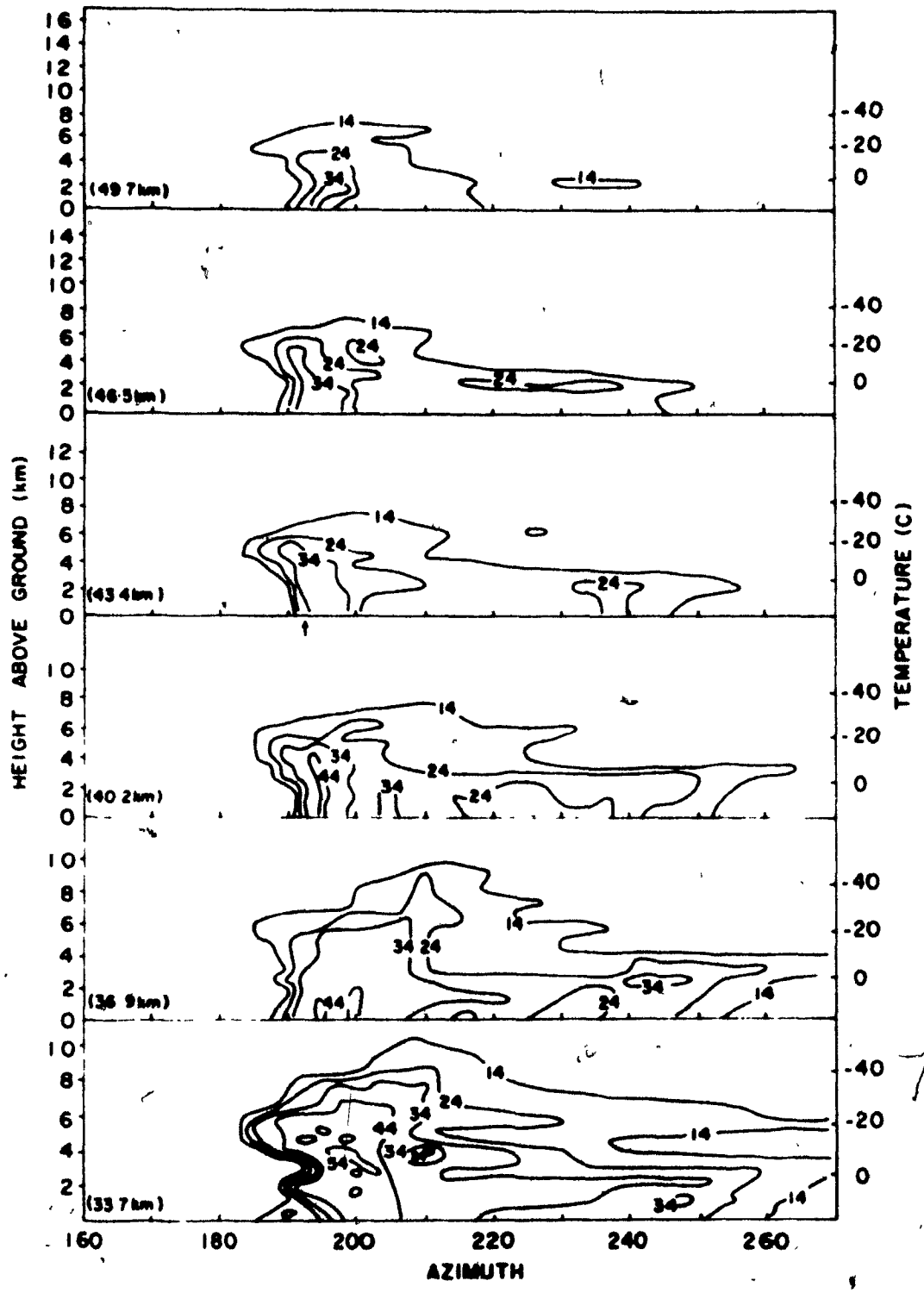

Fig. 6.7 A HARPI display for 1900 MST 28 July 1970. The display is easily understood if one assumes that one is looking SSW towards the storm. The contours of reflectivity are labelled in 10 log Z_e (mm^6 m^{-3}).

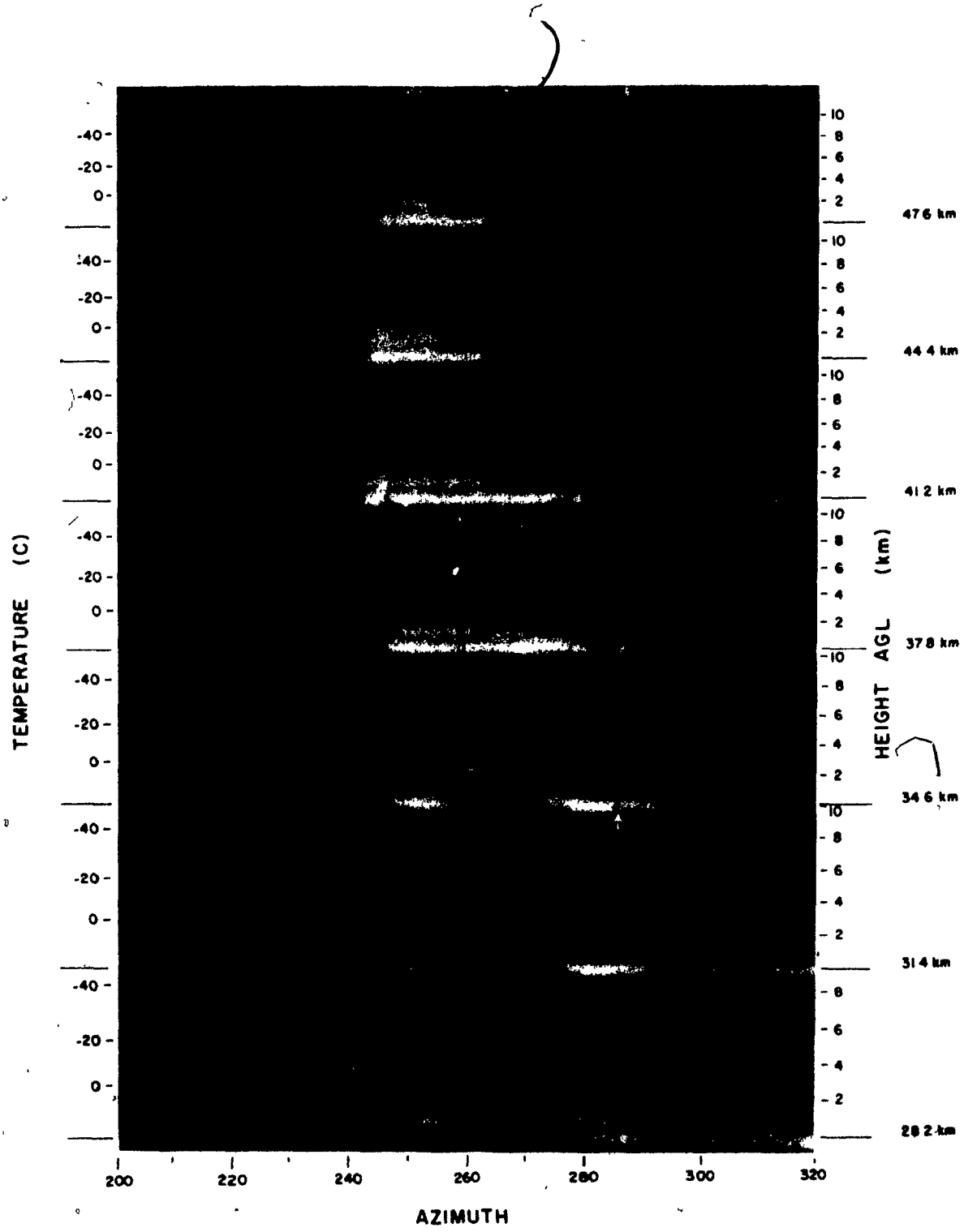

Fig. 6.8 A HARPI display for 1751 MST 3 August 1969. The display is easily understood if one assumes that one is looking west towards the storm.

is indicated by an arrow. Radiosonde data, obtained at the radar site at 1530 MST on both days, provided the indicated temperatures. At the time of the HARPI sections, rainfall at the observing sites of Figs. 6.6a and 6.6b was near its peak value.

The storms of Fig. 6.7 and Fig. 6.8 were moving from 280° and 290° respectively and to the right of the wind vector at middle levels. On the southern edge of both storms, an overhang suggests that an updraft is beneath and inside this portion of the echo, consistent with the arguments of Chisholm (1970) and Marwitz (1971) as developed through extensive measurements in Alberta. There is a large gradient of reflectivity in both storms below the overhang.

The core of the intense precipitation passed to the south of the observing site on 3 August 1969 and north on 28 July 1970. The wind shift was much sharper and the ice nucleus concentration increase during the precipitation was greater on the latter occasion (Fig. 6.6a) than on the former (Fig. 6.6b), although the dewpoint drop of Fig. 6.6b was greater. These differences are probably due to the selection of the sampling location within the storm, rather than any great dissimilarities in structure or radar pattern between the storms.

6.4 DROP-FREEZING MEASUREMENTS

Cumulative concentrations of ice nuclei within rain samples collected in Alberta (Fig. 6.9) were determined by the measurement technique described in section 2.3. This technique is very useful because it specifically detects only immersion-freezing nuclei (see Chapter 5) in actual precipitation samples; the operative nucleation mode is strictly specified. Cloud chamber measurements for some of the time periods indicated in Fig. 6.9 are documented in sections 6.2 and 6.3. For curves A, B, C, E and G, another sample was collected simultaneously about 4 feet away and later analyzed independently by Vali (private

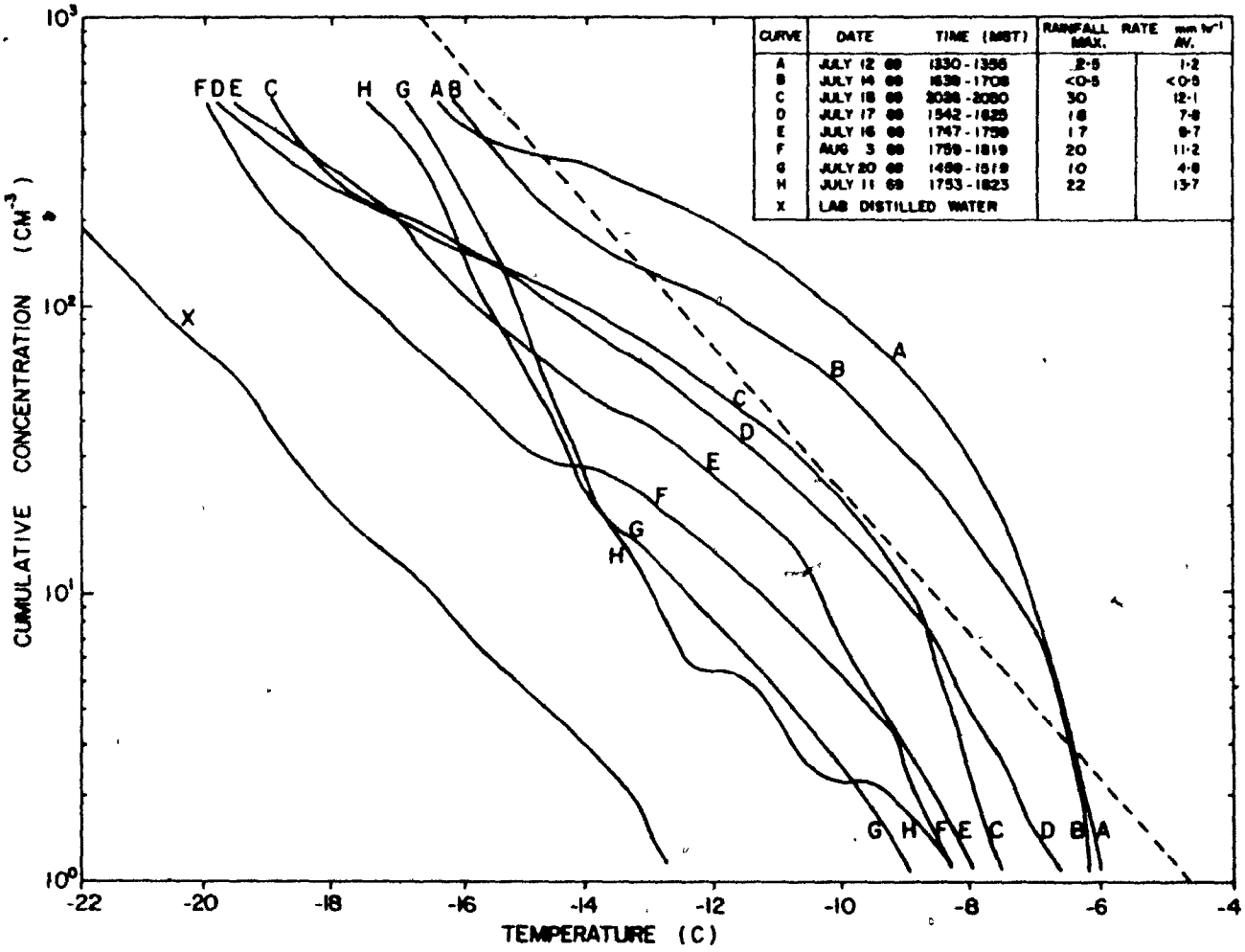

Fig. 6.9 Concentration of ice nuclei in precipitation samples collected at the indicated times. The dashed line is used for calculations described in section 7.2.

communication), and the resultant cumulative concentrations agree with the comparable values of Fig. 6.9 to within a factor of 1.5 for any temperature.

The maximum and average rainfall rate occurring during the collection of each sample is shown in Fig. 6.9 along with the time the collection was made. Sample H represents a mixture of rain and hail (shot to pea-size). Sample F was collected in rain immediately following a hailfall. Although Vali (1971b) has suggested that high rainfall rate samples and hail have higher concentrations of immersion-freezing nuclei, curves H and F, which fulfil either or both of these conditions, are relatively "clean" at temperatures warmer than -15C. The "dirty" samples, A and B, were both collected during low rainfall rates; however, sample B might have contained AgI since the 14 July 1969 storm was seeded (section 6.2).

From this limited number of samples, it appears that precipitation occurring at a very low rainfall rate may have higher concentrations of immersion-freezing nuclei at temperatures warmer than -15C than precipitation occurring at high rainfall rates. This observation is consistent with the data of Engelmann and Perkins (1971) who found that concentrations of ^{39}Cl, a cosmogenic radionuclide, increased with small rainfall rates. Engelmann and Perkins (1971), after summarizing the observations of other authors, conclude that there is a definite inverse relationship between aerosol concentrations in rain and rainfall rate. Rainwater collected during drizzle-like rain might have a longer cloud residence time, thus allowing more aerosol particles to coagulate with the cloud drops (see Chapter 5). This observation of an inverse relation between nucleus concentration and rainfall rate is in disagreement with the measurements of Bishop (1968), but agrees with those of Isaac (1968) for the 28 July 1967 storm. Clearly, interpretation of drop-freezing measurements is difficult.

The cloud chamber results of Figs. 6.2a, 6.2b, 6.2c and Fig. 6.6b can be compared with the droplet-freezing curves H, E, D and F respectively. A higher level of cloud chamber nucleus concentration measurements would show that more nuclei were available to collide with the precipitation. The concentrations of Figs. 6.2b and 6.2c are at least a factor of 10 apart during their respective precipitation sample collection times, but the corresponding curves, E and D of Fig. 6.9, are very similar. Extensions of the curves H and F would be almost a factor of 10 apart at -20C but at the corresponding collection times in Figs. 6.2a and 6.6b, the ice nucleus chamber concentrations are almost the same. There appears to be no correlation between the immersion-freezing nucleus concentrations of Fig. 6.9 and the NCAR Ice Nucleus Counter measurements during the respective sample collection period. Considering the nuclei-droplet coagulation problems mentioned in Chapter 5, this lack of correlation should not be unexpected.

6.5 POSSIBLE EXPLANATIONS OF THE OBSERVATIONS

A few possible causes for ice nucleus concentration increases associated with the thunderstorms of sections 6.1, 6.2 and 6.3 are discussed below.

1) Air entering the storm through the updraft, or due to entrainment, could have contained large concentrations of ice nuclei. However, the updraft air would probably mix with the surface layer, and ground measurements would show a gradual increase before the storm.

2) Ice nuclei might be concentrated into the thunderstorm downdraft. Ice nuclei in the incoming air could be trapped in the storm when they initiated drop or crystal formation themselves, or by coagulation with existing precipitation. When this precipitation falls out, and drops evaporate, they would enrich the surrounding air by releasing ice nuclei. The fact that peaks in ice nucleus

concentration do not always coincide with rainfall rate maximums creates a problem for the above hypothesis.

3) Particles placed in the downdraft might be preactivated ice nuclei. However, it is unlikely these nuclei could survive in the warm surface air.

4) High winds in the vicinity of thunderstorms blow up dust which could be a good source of nuclei. This hypothesis has been strongly advocated by Rosinski et al. (1971), and Vali (1968) has shown that soil is a relatively good nucleating material. However, both in Quebec and Alberta, on dry days with high winds no great increases in nucleus concentration are observed. During thunderstorms the additional inhibition of a wet ground surface would retard any dust pickup by the wind.

5) An unusual change in a meteorological parameter, such as relative humidity or temperature, in the downdraft might enhance the activity of the nuclei. No evidence was collected to support this hypothesis, but a change in the above parameters might modify the cloud characteristics in the cloud chamber, and according to Chapter 5, change the measured concentration. Temperatures within the chamber were monitored and did not vary. An artificial source of condensation nuclei kept the cloud drop concentration constant. The dewpoint temperature drop during thunderstorms might reduce the liquid water content in the chamber, but this would reduce the nuclei-droplet coagulation efficiency (mentioned in Chapter 5) and possibly the ice nucleus concentrations. The observations show the concentration increases; the variations are not due to instrumental reasons.

6) Gabarashvila and Kartsivadze (1968, 1969) discuss how both electric field and electric charges influence ice nucleus formation. In a thunderstorm, some electrical mechanism such as lightning, by charging particles or creating

new ones, could either produce more ice nuclei or more effective nuclei.

Isono and Tanaka (1966), Ryan and Scott (1969) and Rosinski et al. (1971) suggest that the first, second and fourth mechanisms respectively are the primary causes of nucleus concentration increase during a thunderstorm. The first two papers mentioned above each contained one storm example with less detailed data than any of the Alberta or Quebec storms documented in this thesis. Rosinski et al. (1971) state that "concentrations of ice-forming nuclei, which derive from soil particles, increase during storms up to 100 times the pre-storm value". Some of their data are similar to that in Fig. 6.1, although their data are not as detailed (time resolution). The theory of Rosinski et al. (1971) is attractive, but some of the above observations illustrate difficulties with such a hypothesis.

Based upon data in this thesis, one can only conclude that large increases in surface ice nucleus concentrations are observed during storm precipitation. One cannot state that the storm existed within a region of higher ice nucleus concentrations or that it created the condition. Ragette (1971), using pibal observations in and around Alberta hailstorms, has concluded that downward motions exist throughout most of the radar echo region. The downdraft core was usually located in the rear portion of the echo, although it was once situated in the central portion of the echo. From the observations of Ragette, it appears that the high ice nucleus concentrations occur in the storm downdraft. The observation of Ragette, that the downdraft core is usually in the rear portion of the radar echo, would explain the tendency for the maximum concentration to occur after the rainfall rate maximum (see Figs. 6.1a, 6.2a and 6.3). Figs. 6.6a and 6.6b support the hypothesis that the ice nucleus concentrations increase during the storm downdraft; in these cases, the increase occurred with the arrival of the gust front (downdraft air). Fig. 6.4 suggests that AgI

released aloft was brought to the surface in a downdraft occurring during the precipitation.

There does not appear to be any difference between hailing and non-hailing storms in terms of the intensity of the ice nucleus concentration fluctuations near -20C. This can be seen by comparison of Fig. 6.1 with Figs. 6.6 and 6.2a, if one remembers that the concentration increases by a factor 10 for a 4 degree drop in chamber temperature (Mason, 1968). The Alberta storm concentrations are very similar to the values obtained in Quebec during storms.

Curves D and B of Fig. 4.2 are not directly comparable because D was obtained during the winter in Quebec while B is formed from summer measurements. However, from 29 July 1971 to 2 August 1971 the geometric mean concentration of 372 samples, each of 150 litres in size, at Macdonald College, Quebec was 0.28 per litre at -21C. Using this short-term measurement of only 4 days, there is no difference between summer and winter concentrations in Quebec. The summer measurements show that Quebec concentrations might be a factor 2 higher than in Alberta. This difference is not considered significant when compared with a geometric standard deviation of 3. Consequently, there is no evidence to suggest that ice nucleus concentrations or fluctuations at -20C in Alberta and Quebec are different.

6.6 A POSSIBLE FEED-BACK MECHANISM IN CONVECTIVE STORMS

Could the increases in ice nucleus concentration feed back and influence the storm itself? This question is a real one if high ice nucleus concentrations in the downdraft mix with the updraft and thus affect the storm.

For example, Fig. 6.10 shows the 43.4 km HARPI section for 28 July 1970 at 1900 MST (reproduced from Fig. 6.7). The data of Fig. 6.6a were obtained at the position indicated by the arrow. The position of the gust front F at 1900 MST was estimated by assuming the gust front passed the site at approximately 1830 MST moving at the storm velocity of 4.5 m sec^{-1} from 280°. The height of

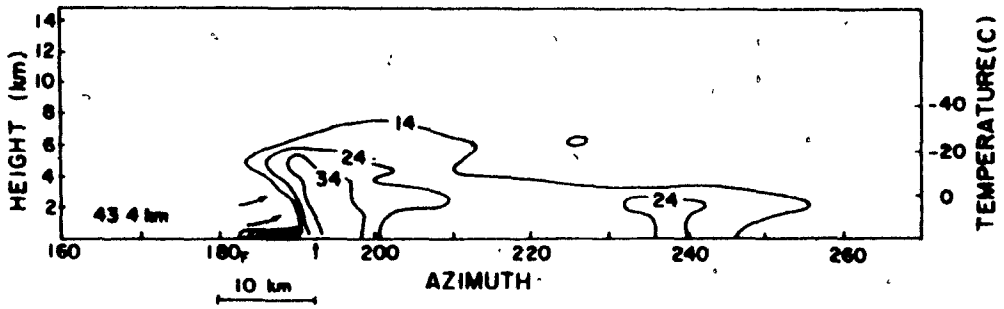

Fig. 6.10 The 43.4 km HARPI section of Fig. 6.7. The updraft and downdraft are indicated by the arrows. F indicates the surface position of the gust front, while the hatched area represents the cold dome or air spreading out underneath the storm. The observation site for Fig. 6.6a is marked by the vertical arrow.

the cold dome (hatched area) was taken to be several thousand feet as observed by Byers and Braham (1949). Arrows are drawn to indicate the updraft and cold dome air flow in the plane of the section.

For any storm similar to Fig. 6.10, the observed higher concentration of nuclei at the surface gust front would probably mix with the updraft air ahead of the storm. If it is assumed that air within the whole vertical extent of the cold dome (instead of just at the surface) contains higher concentrations of ice nuclei, then this nucleus-rich air would mix with the updraft air all along the updraft-downdraft shear zone aloft. Chapter 7 examines what would happen to the ice content of the updraft if this situation occurred. The data of Figs. 6.6a and 6.6b indicate that, at least for a considerable fraction of the time, it is likely that the greater concentrations in the downdraft mix into the storm updraft.

CHAPTER VII

THE ICE CONTENT OF A SEVERE STORM UPDRAFT

Three different methods of evaluating the rate of production of ice within a storm updraft will be described in this chapter. Jiusto (1968) (section 7.1) has calculated the critical concentration necessary to increase the ice/water concentration ratio. Using the drop-freezing technique of section 2.3, and known cloud-drop sizes, the fraction of water frozen in a cloud can be estimated (section 7.2). These two methods will be compared with the ice content estimated by activating ice nuclei according to a specified nucleus concentration versus temperature relation, and then growing the crystals by sublimation in a severe storm updraft (section 7.3).

7.1 CRITICAL CONCENTRATION OF ICE NUCLEI

According to Fletcher (1962) the supersaturation (S) in a convective cloud can be specified as:

$$\frac{dS}{dt} = Q_1 v - Q_2 \frac{dm}{dt}$$

where Q_1 and Q_2 are thermodynamic functions evaluated by Squires (1952), v is the updraft velocity, and $\frac{dm}{dt}$ is the condensation rate. If $\frac{dS}{dt}$ equals zero, then

$$\frac{dm}{dt} = \frac{Q_1}{Q_2} v .$$

The growth rate of an ice crystal by diffusion (Fletcher, 1962) is given by:

$$\frac{dm_c}{dt} = 4\pi C G' S_i \rho_i$$

where G' is a thermodynamic function, S_i is the supersaturation with respect to ice, and ρ_i and C are the ice density and crystal shape factor respectively. If the supply rate of moisture to the cloud equals the extraction rate due to N_c

T (C)	Q_1/Q_2 (gm cm^{-4})	Vapour supply dm/dt (gm sec^{-1} cm^{-3})	Critical ice nuclei N_c (l^{-1})
- 5	1.285×10^{-11}	6.42×10^{-10}	340
-10	1.045	5.23	180
-20	0.623	3.12	105
-30	0.323	1.62	85
-40	0.147	0.735	80

Table 7.1 Critical concentration of ice nuclei (N_c) required for the ice/water concentration ratio to increase. The crystal radii and updraft velocity are assumed to be 100 μm and 50 cm sec^{-1} respectively. (After Jiusto, 1968)

plane dendrite crystals ($C = \frac{2r}{\pi}$) growing by sublimation, then

$$N_c = \frac{Q_1 v/Q_2}{8G'S_i\rho_i r}$$

If there is one crystal created per ice nucleus activated, then N_c represents the critical concentration of nuclei needed for the ice/water concentration ratio to increase. Jiusto (1968) has computed N_c for an updraft velocity of 50 cm sec^{-1} and a plane dendrite crystal of radius 100 μm; his results are presented in Table 7.1. At -20C one needs approximately 100 crystals per litre, and if the updraft velocity is increased to 10 m sec^{-1}, 2000 per litre are required. The critical concentration of crystals increases if the crystal size is reduced. Normally there is one ice nucleus per litre at -20C (Mason, 1968). Since the concentration of ice nuclei increases by a factor 10 for every 4C drop in temperature, the ice nucleus concentration would approach the critical concentration of Table 7.1 near -30C. In an updraft of 10 m sec^{-1}, with a realistic crystal diameter of 20 μm, one would need 2×10^4 times normal background ice nucleus concentration in order for the critical concentration to occur at -20C.

7.2. THE DROP-FREEZING ESTIMATE OF THE ICE CONTENT

The total number of drops frozen in a cloud can be estimated using the results of the drop-freezing experiments described in section 2.3 and assuming the droplets have a volume V. Using Eq. (2.1), the fraction f(T) of drops frozen within a cloud can be specified as Vali (1968):

$$f(T) = \frac{N(0) - N(T)}{N(T)} = 1 - \exp[-VK(T)] .$$

By specifying K(T) as in the dashed line of Fig. 6.9

$$K(T) = C_1 \exp[0.576(273 - T)]$$

C_1 (nuclei cm^{-3})	-44C	-40C	-36C	-32C	-28C	-24C	-20C
7.14×10^{-3}	0.95	0.26	0.03	0.003	0.0003	0.00003	0.000003
7.14×10^{-2}	1.0	0.95	0.26	0.03	0.003	0.0003	0.00003
7.14×10^{3}	1.0	1.0	1.0	1.0	1.0	1.0	0.95

Table 7.2 Fraction of drops (20 μm) frozen for a few values of temperature and C_1.

where C_1 equals 7.14×10^{-2} nuclei cm^{-3}. For a drop diameter of 20 μm, Table 7.2 indicates the fraction frozen for seven temperature levels as well as three values of C_1. The two lower values of C_1 cover the range of concentrations of Fig. 6.9. Increasing the drop diameter by a factor $10^{1/3}$ has the same effect as increasing C_1 by a factor 10. From Table 7.2, it is apparent that in order to freeze the entire cloud at -20C, one would need a value of 7.14×10^3 for C_1 or 10^5 times the number of immersion-freezing nuclei per cm^3 specified by the dashed line of Fig. 6.9.

7.3 UPDRAFT ICE CONTENT VERSUS HEIGHT

There are a few defects in the models of sections 7.1 and 7.2. The critical concentration method of Jiusto suffers because the crystal size must be specified, and in a severe storm updraft where time is limited, a realistic value is difficult to estimate. Although the rate of moisture supply equals the extraction at critical concentration, the time required to freeze the entire cloud may be significant. The drop-freezing technique does give an estimate of the ice content, but it is not directly dependent upon updraft velocity. If the assumed cloud droplet radius were held constant, an updraft of 1 cm sec^{-1} would glaciate at the same level as a severe storm updraft. The drop-freezing model does not consider the effect of already-frozen drops growing either by sublimation or accretion.

A simple model was developed to help solve some of the above problems. A parcel of air was assumed to rise at 10 m sec^{-1} in a water-saturated environment with a lapse rate of 6.6C km^{-1}. The melting level (0C) was taken to be 650 mb. Spherical crystals grew by diffusion according to:

$$\frac{dM_c(T_o,T)}{dt} = \left[\frac{4\pi D(T)\,\rho_v/\rho_s}{1 + \frac{D(T)\,L^2\rho_v M_w}{RT^2 K(T)}}\right] \cdot \left[\frac{P_w(T)}{P_i(T)} - 1\right] \cdot \left[\frac{3}{4\pi\rho_s}\right]^{1/3} \cdot M_c(T_o,T)^{1/3} \quad \ldots (7.1)$$

(Fletcher, 1962)

where:

$M_c(T_o,T)$ = mass of crystal (activated at T_o) at temperature T

T = temperature

$P_w(T)$ = saturation vapour pressure over water at temperature T

$P_i(T)$ = saturation vapour pressure over ice at temperature T

R = universal gas constant

D(T) = diffusivity of water vapour in air

L = latent heat of sublimation

ρ_s = density of ice (0.9 gm cm^{-3})

ρ_v = density of vapour

M_w = molecular weight of water

t = time

The initial radius was assumed to be 1 μm. The number $N(T_o)$ of ice nuclei activated in a specific 1C temperature interval was determined from:

$$N(T_o) = 8.7 \times 10^{-3} [\exp(0.576) - 1] \exp[0.576(272.5 - T)] \quad (7.2)$$

nuclei/kg

which was calculated using the assumptions that there exists 1 nucleus per litre at -20C and 900 mb and that the concentration increases by a factor 10 for every 4C drop in temperature. These assumptions form the basis for the generally accepted ice nucleus spectrum between -10C and -30C (Mason, 1968; see also Fig. 1.1). The assumed concentration at -20C does not correspond to the values presented in Fig. 6.2 and Fig. 6.6 or Fig. 4.2, but the NCAR Ice Nucleus Counter is assumed to produce a low reading and consequently, the more acceptable standard of 1 per litre found around the world has been adopted.

The ice content $I_c(T)$ at a specific temperature T in the updraft can be expressed as:

$$I_c(T) = \sum_{T_o=0}^{T} M_c(T_o,T)\, N(T_o) \text{ gm/kg} \quad (7.3)$$

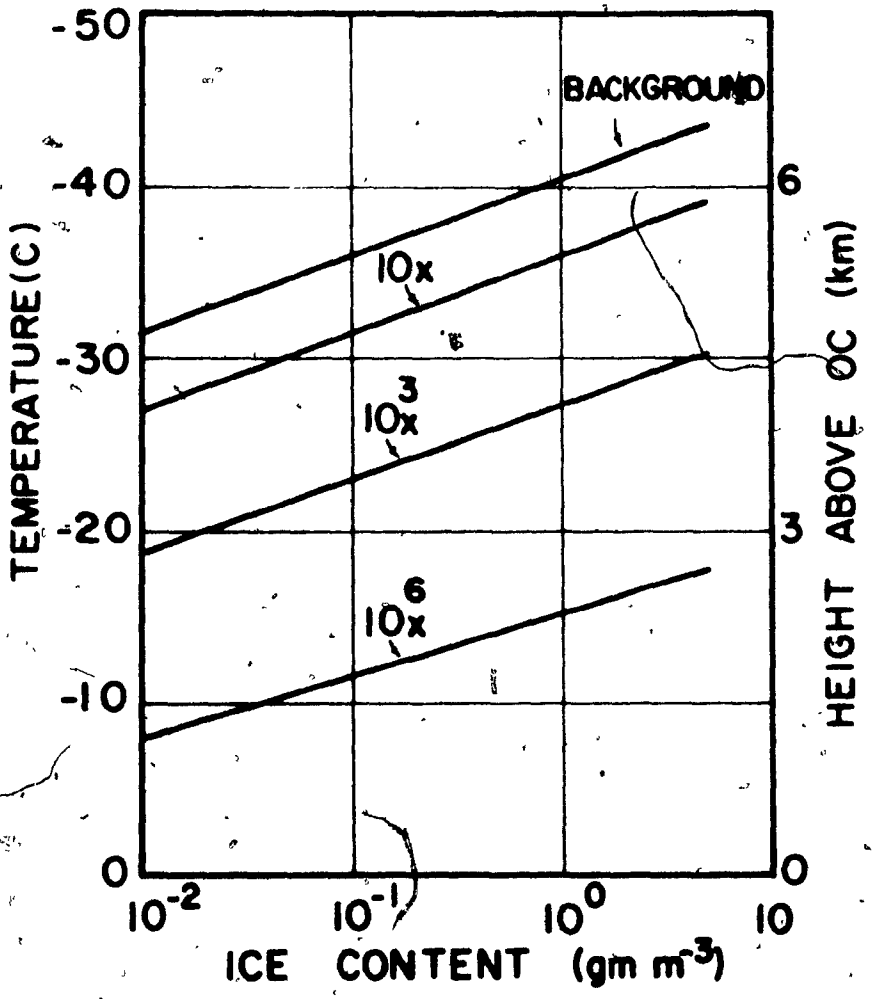

Fig. 7.1 Ice content $I_c(T)$ of an updraft of 10 m sec^{-1}. Each curve represents a different ice nucleus concentration vs temperature relation. When $I_c(T)$ approaches the cloud liquid water content, the model becomes meaningless.

Fig. 7.1 shows the results of a computer solution of Eq. (7.3) obtained by integrating Eq. (7.1) for time steps equivalent to 1C temperature intervals. $I_c(T)$ has been converted into the more useful units of gm m^{-3}. The curve labelled "background" shows the amount of ice the cloud would contain using the nucleus spectrum of Eq. (7.2). The curves labelled 10, 10^3, and 10^6 indicate the ice content when the background ice nucleus concentration (1 nucleus per litre at -20C) is multiplied by this factor. These curves represent seeded updrafts.

The above model (Eq. 7.3) can be clarified by introduction of the following four relations:

$$\frac{dT}{dz} = -K_1 \qquad (a)$$

$$N = N_o e^{-K_2 T} \qquad (b) \qquad (7.4)$$

$$\frac{dz}{dt} = v \qquad (c)$$

$$\frac{dM}{dt} = K_3 M^{1/3} \qquad (d)$$

K_1, K_2 and K_3 are constants, v is the updraft velocity, z is the height above the 0C level, M is an individual crystal mass, and N represents the concentration of nuclei active at temperature T (Celsius) or above. N_o is equivalent to the value of 8.7×10^{-3} in Eq. (7.2), if K_2 equals 0.576. Eqs. (7.4) lead to the following:

$$I_c(z) = \frac{3\sqrt{\pi}}{4} \left(\frac{2K_3}{3vK_1K_2}\right)^{3/2} N_o e^{K_2 K_1 z} \qquad (7.5)$$

Eq. (7.5) differs from Eq. (7.3) (used for the computer solution) only in that K_3 is assumed constant. Since over the temperature range -1OC to -4OC, K_3, as defined by Eq. (7.1), varies by only a factor of 1.5, this assumption does not introduce large errors in the computation of I_c.

As Eq. (7.3) and Fig. 7.1 show, increasing $N(T_o)$ for all T_o by a factor of 10 simply increases the ice content I_c at a specific temperature level tenfold. This observation is independent of the assumptions used in computing $M_c(T_o,T)$ and of the value of 0.576 used in the exponent of $N(T_o)$. The ice content for each curve of Fig. 7.1 increases exponentially with height. Not only does the approximation Eq. (7.5) verify the two above conclusions, but this equation predicts that an increase in updraft velocity by a factor of 100 would decrease the ice content at any level by a factor of 1000. Further computer calculations have shown that this prediction is valid when K_3 is not held constant but is specified as in Eq. (7.1).

The height at which a given concentration of ice is obtained (Fig. 7.1) decreases by approximately 0.75 km (i.e. 4.5C) for each tenfold increase in nucleus concentration. The ice content at any level in Fig. 7.1 is directly proportional to the ice nucleus concentration at any temperature (Eq. 7.3).

7.4 MODEL ASSUMPTIONS

Many variables used in the model of section 7.3 (such as updraft velocity, the lapse rate, the value of 0.576 in Eq. (7.1), supersaturation, and the crystal shape (spherical) and density) have been assumed constant and independent of temperature or height. Cloud droplets were not allowed to freeze, and crystal growth by accretion was neglected. Most of the above assumptions were checked to test whether their inclusion radically changed the results of the model.

The loaded moist adiabatic updraft velocities determined by Chisholm (1970) usually increase from the melting level but rarely exceed a factor of 2 or 3 of the -5C value. Since 10 m sec^{-1} (used in Fig. 7.1) is a typical value for the storm updraft core between 0C and -5C for either a small, medium or high

energy storm (Chisholm, 1970), the updraft at lower temperatures would be slightly higher. Eq. (7.5) predicts that if the updraft velocity between -5C and -40C was up to a factor of 3 higher, the ice content at these temperatures would decrease by a maximum of a factor of $3^{3/2}$.

The value of 0.576 in Eq. (7.2) was obtained by assuming that the ice nucleus concentration increased by a factor of 10 for a 4C drop in temperature. Fig. 1.1 shows this is a reasonable assumption for North America, and Isaac (1968) showed that ice nucleus concentrations in Quebec followed a similar temperature dependence between -15C and -30C. Some ice nucleus temperature spectra obtained in Alberta in 1970 suggest a factor of 10 increase for a 3C drop in temperature between -15C and -30C. Holding the concentration at -20C constant, Eq. (7.5) predicts that if the temperature dependence took the form of a tenfold increase in concentration for a 3C or a 5C drop in temperature, the ice content at -40C would increase by a factor of 30 and decrease by a factor of 7 respectively from the values of Fig. 7.1, while that at -20C would remain within a factor of 2. The assumed nucleus concentration at -20C would still have to be increased by a factor 10^5 in order to completely glaciate the cloud. A serious difficulty in the selection of the value of 0.576 in Eq. (7.1) is the lack of measurements between -30C to -40C where ice contents become appreciable; measurements from -10C to -30C must be extrapolated to lower temperatures. The drop-freezing technique for determining "fraction frozen" also suffers from this lack of data.

The air was assumed to be saturated with respect to water. Although in a severe storm updraft slightly supersaturated air with respect to water can be expected, the value of supersaturation with respect to ice would not be modified enough to significantly affect the crystal growth rate. In a severe

Alberta storm, the concentration of water and ice combined can range from 2.5 gm m^{-3} to 5 gm m^{-3} (Chisholm, 1970). When the value of ice content in Fig. 7.1 approaches this combined ice and water concentration, the air will no longer remain saturated with respect to water but will approach saturation with respect to ice; at this point the model becomes meaningless.

For a given value of ice content, the ice crystal size distribution is approximately the same for any of the curves of Fig. 7.1. If the slope of the background curve of Fig. 7.1 changes at a particular value of $I_c(T)$, due to coagulation or splintering of the crystals or even depletion of the cloud water (resulting in unsaturated air with respect to water), the 10x-curve would change by an equal amount at the same value of ice content; the two curves would maintain the same separation. Coagulation or splintering of the crystals, or even depletion of the cloud water, would not greatly affect the conclusion that the height at which a specific ice content is obtained decreases by 0.75 km for a factor 10 increase in nucleus concentration.

The above model considered sublimational growth of spherical crystals. Another model was used, in which the crystals were planar, and growth was by riming as well as by sublimation. The following mass-size relationships were used, following Nakaya and Terada (1934):

Crystal Type	Mass-Size Relation
1. Planar unrimed	$r_c = (m_c/0.00152)^{1/2}$
2. Partially rimed	$r_c = (m_c/0.0108)^{1/2}$
3. Heavily rimed	$r_c = (m_c/0.52)^{1/3}$

m_c and r_c are the crystal mass (gm) and radius (cm) respectively, and appropriate expressions for growth rates by riming or sublimation (Jiusto, 1971) were used. Planar unrimed crystals were grown exclusively by sublimation. When

the calculated growth rate for accretion exceeded that for sublimation, growth proceeded by riming alone, assuming the second mass-size relation listed above and a liquid water content of 5 gm m^{-3}. After the crystal mass reached 4×10^{-3} gm, riming growth continued using the third mass-size relation above. The terminal crystal velocities were calculated using an expression derived by Langleben (1954). Jiusto (1971) has used the above model, with the three crystal mass-size relations, to describe crystal development and glaciation in a layer cloud with a constant temperature. His restrictions were relaxed in this study; the crystals were assumed to be growing in a water saturated parcel rising at 10 m sec^{-1} with ice nuclei being activated according to Eq. (7.2).

At -40C, crystals which had activated between -1C and -11C were "heavily rimed", those activated between -12C and -27C were "partially rimed", and the rest were still growing by sublimation. The greatest concentration of ice mass was due to crystals still growing by sublimation, because they were far more numerous. The curves of Fig. 7.1 remain valid since, using the above model, $I_c(T)$ would increase less than 10 percent for all heights; thus, growth by riming can be neglected in the calculation of the ice content of the updraft. However, crystals grew as large as 0.5 cm in diameter, with an estimated fall velocity of 1.3 m sec^{-1}. The model of Fig. 7.1 cannot be extended to low updraft velocities where crystals grow large enough to start falling out of the cloud.

7.5 SUMMARY

Two useful conclusions, which do not depend critically on the assumptions, can be obtained from the model of Fig. 7.1.

1.) The updraft ice content at any level or temperature is directly proportional to the concentration of ice nuclei.

2.) To completely freeze all the water at -20C, in an updraft of 10 m sec^{-1} with an adiabatic liquid water content of 5.0 gm m^{-3}, the normal background concentration of nuclei must be increased by a factor between 10^5 and 10^6.

Since the increase in concentration observed in the storm downdrafts (described in Chapter 6) was never much more than a factor of 10, mixing the updraft and downdraft air would increase the updraft ice nucleus content by a smaller factor; according to Fig. 7.1, the ice content at any temperature level would not change more than tenfold.

Because the higher nucleus concentrations in the downdraft might later mix with the updraft, the growth of hail could be affected. English (1972) has shown that, for a medium energy storm (Chisholm, 1970), decreasing the "freezing level" by 5C would reduce the diameter of hail which had trajectories reaching -35C by more than a factor of 2 in diameter. The largest hail never reaches the -35C level and remains uninfluenced. To reduce hail completely, all the cloud water must freeze by -20C in a medium energy storm. It is unlikely that a factor of 10 increase in ice nucleus concentration within the updraft would freeze enough cloud water to dramatically affect hail production. The effect on weaker storms might be more pronounced. The concentration of hail embryos might increase, but this possibility has not been studied.

Fig. 7.1 indicates that in order to freeze all the cloud water at -20C in a 10 m sec^{-1} updraft, one would have to supply between 10^5 and 10^6 times the normal concentration of nuclei. The drop-freezing technique (section 7.2) indicates that the nucleus concentration in the cloud droplets would have to be increased by the same amount. The critical concentration method (section 7.1) predicts that 2×10^4 times background is necessary for the ice/water concentration ratio to increase at -20C.

CHAPTER VIII

CONCLUSIONS

This chapter briefly summarizes conclusions which have been described in sections 4.5, 5.4, 6.5 and 7.5. These and other appropriate sections are referenced in the following discussion.

Ice nucleus concentrations near -20C have been measured with an NCAR Ice Nucleus Counter; although this instrument has many defects, measurements described in section 4.1 indicate that the magnitude of fluctuations in concentration is similar to data obtained using other techniques. Four different types of ice nucleus counters produce log-normal distributions of ice nucleus concentrations, with approximately the same geometric standard deviation, when measurements are made over a sufficiently long period such as several weeks. Over periods of one to three hours, when the concentration appears steady, the theoretically expected Poisson distribution was found to fit the data (section 4.2). Many meteorological parameters are distributed log-normally; for example, it was found that frequency distributions of hail-fall rates, hailstone dimensions and radar reflectivities of hail samples were log-normal (section 4.3).

In Chapter 5 it was shown that aerosols of ice nucleus size require a considerable time to coagulate with cloud drops. Ice nucleus cloud chamber counters, with short cloud residence times, might seriously underestimate concentrations of immersion-freezing or contact-freezing nuclei which would activate in long lasting stable atmospheric clouds. However, these cloud chambers probably estimate realistically the number of ice nuclei activated in severe storm updrafts (section 5.4).

Large increases (factor of 10 or higher) in ice nucleus concentrations at -20C are measured during precipitation in Quebec and Alberta thunderstorms. Ragette (1971) states that downdrafts are present in the precipitation region of Alberta storms and evidence was presented in Chapter 6 to show that the observed high ice nucleus concentrations are associated with these downdrafts. Variations in ice nucleus concentrations and the level of concentration are similar in both Alberta and Quebec thunderstorms and for hailing and non-hailing storms (section 6.5).

No evidence was found to suggest that ice nucleus concentrations in Alberta and in Quebec (at -20C) differ significantly either in absolute magnitude or in the scale of fluctuations. Hour-to-hour variations can be greater than any slight difference in long term means of concentrations between the two provinces (section 6.5).

If the higher ice nucleus concentration in a storm downdraft mixes with the storm updraft, no dramatic change in ice content of the updraft core is to be expected (section 7.5). A tenfold increase in ice nucleus concentration would increase the ice content at any level by the same proportion; the level at which any given ice content is found is lowered by 0.75 km. In order to seed a storm updraft of 10 m sec^{-1} and completely glaciate the cloud by -20C, 10^5 to 10^6 times the normal background concentration of ice nuclei is required. These conclusions were obtained from the model developed in section 7.3; calculations using the drop-freezing model of section 7.2 and the critical concentration method of section 7.1 indicate that these conclusions are reasonable.

REFERENCES

Aitchison, J., and J.A.C. Brown, 1957: The Lognormal Distribution. London, Cambridge University Press, 176 pp.

Alkezweeny, A.J., 1971: A contact nucleation model for seeded clouds. J. Appl. Meteor., 10, 732-738.

Auer, A.H., 1967: Characteristics of the cloud within the NCAR Nucleus Counter. Univ. of Wyoming Information Circular, No. 51.

-----, D.L. Veal, and J.D. Marwitz, 1969: Observations of ice crystals and ice nucleus concentrations in stable cap clouds. J. Atmos. Sci., 26, 1342-1343.

Barge, B.L., 1971: Hail Detection with a Polarization Diversity Radar. Ph.D. Thesis, Dept. of Meteor., McGill University, Montreal.

-----, and G.A. Isaac, 1970: Shape, size and surface characteristics of hailstones collected in Alberta. Proc. Conf. Cloud Physics, Fort Collins, 83-84.

Bigg, E.K., 1957: A new technique for counting ice-forming nuclei in aerosols. Tellus, 9, 394-400.

-----, 1961: Natural atmospheric ice nuclei. Science Progress, 49, 458-475.

-----, 1965: Problems in the distribution of ice nuclei. Proc. Intn'l. Conf. Cloud Physics, Tokyo, 137-140.

-----, 1970a: Comments on "Ice nucleus measurements at three sites in western Washington." J. Atmos. Sci., 27, 1218-1219.

-----, 1970b: Report on the ice nucleus workshop, Fort Collins. Proc. Ice Nucleus Workshop. In press at Colorado State University.

-----, and R.T. Meade, 1959: Continuous automatic recording of ice nuclei. Bull. Obs. Puy de Dome, 4, 125-138.

-----, and G.T. Miles, 1964: The results of large-scale measurements of natural ice nuclei. J. Atmos. Sci., 21, 396-403.

-----, and C.M. Stevenson, 1970: Comparisons of concentrations of ice nuclei in different parts of the world. J. Rech. Atmos., 4, 41-58.

-----, S.C. Mossop, R.T. Meade, and N.S.C. Thorndike, 1963: The measurement of ice nucleus concentrations by means of Millipore filters. J. Appl. Meteor., 2, 266-269.

Bishop, D.D., 1968: Temperature Spectra of Freezing Nuclei in Precipitation. M. Sc. Thesis, Dept. of Meteor., McGill University, Montreal.

Bowen, E.G., 1958: Freezing nucleus measurements in January, 1957. Aust. J. Physics, II, 452.

Buscaglione, A., 1968: Ice nuclei measurements in Italy--some results. Proc. Intn'l. Conf. Cloud Physics, Toronto, 227-231.

Byers, H.R., and R.R. Braham, 1949: The Thunderstorm. U.S. Gov't. Printing Office. Wash. 25, D.C., 287 pp.

Chisholm, A.J., 1970: Alberta Hailstorms: A Radar Study and Model. Ph.D. Thesis, Dept. of Meteor., McGill University, Montreal.

Cotton, W.R., 1970: A numerical simulation of the growth of a system of ice crystals in small convective clouds. Proc. 2nd National Conf. Wea. Mod., Santa Barbara, 24-28.

Crozier, C.L., 1969: An Expansion Chamber Technique for Determining Ice Nucleus Concentration. Canadian Meteor. Research Report. 50 pp.

Davis, M.H., and J.D. Sartor, 1967: Theoretical collision efficiencies for small cloud droplets in Stokes flow. Nature, 215, 1371-1372.

Douglas, R.H., 1963: Size distributions of Alberta hail samples. Sci. Rep. MW-36, Stormy Weather Research Group, McGill University, Montreal, 55-70.

-----,1965: Size distributions of Alberta hail samples. Sci. Rep. MW-42, Stormy Weather Research Group, McGill University, Montreal, 45-47.

Dufour, L., 1966: Noyaux glacogene dans l'atmosphere. Ciel et Terre, 82, 1-34.

Engelmann, R.J., and R.W. Perkins, 1971: Precipitation processes revealed by cosmogenic radionuclide scavenging. J. Atmos. Sci. 28, 131-133.

English, M., 1972: The Growth of Large Hail. Ph.D. Thesis, Dept. of Meteor., McGill University, Montreal.

Fenn, R.W., and H.K. Weickmann, 1959: Some results of aerosol measurements. Geofis. Pur. Appl., 42, 53.

Fisz, M., 1963: Probability Theory and Mathematical Statistics. New York, John Wiley and Sons, 677 pp.

Fletcher, N.H., 1958: Time lag in ice crystal nucleation in the atmosphere, Part 2, Theoretical. Bull. Obs. Puy de Dome, No. 1, 11-18.

Fletcher, N.H., 1962: The Physics of Rainclouds. Cambridge, Cambridge University Press, 386 pp.

Gabarashvili, T.G., and A.I. Kartswadze, 1968: Influence of electric field upon processes of ice nucleus formation. Proc. Intn'l. Conf. Cloud Physics, Toronto, 188-193.

-----, 1969: Influence of electric charges upon the ice forming activity of artifical nuclei. Proc. 7th Intn'l. Conf. Condensation and Ice Nuclei, Prague and Vienna, 220-224.

Gagin, A., 1965: Ice nuclei, their physical characteristics and possible effect on precipitation initiation. Proc. Intn'l. Conf. Cloud Physics, Tokyo, 155-162.

-----, 1971: Studies of the factors governing the colloidal stability of continental cumulus clouds. Proc. Conf. Wea. Mod., Canberra, 5-11.

-----, and M. Aroyo, 1969: A thermal diffusion chamber for the measurements of ice nuclei concentrations. J. Rech. Atmos., 4, 115-122.

Georgii, H., 1960: The influence of climate and weather elements on the activity of natural freezing nuclei. Physics of Precip. Geophys. Mono., 5, 233-239.

Gerber, H.E., P.A. Allee, H.K. Weickmann, U. Katz, C.I. Davis and L.O. Grant, 1970: Some size distribution measurements of AgI nuclei with an aerosol spectrometer. J. Atmos. Sci., 27, 1060-1067.

Goldsmith, P., H.J. Delafield, and L.C. Cox, 1963: The role of diffusiophoresis in the scavenging of radioactive particles from the atmosphere. Quart. J. Roy. Meteor. Soc., 89, 43-61.

Grant, L.O., 1968: The role of ice nuclei in the formation of precipitation. Proc. Intn'l. Conf. Cloud Physics, Toronto, 305-310.

Greenfield, S.M., 1957: Rain scavenging of radioactive particulate matter from the atmosphere. J. Meteor., 14, 115-125.

Guenadiev, N., 1970: Sur le mecanism de congelation des gouttes d'eau sous l'influence d'un aerosol d'iodure d'argent. J. Rech. Atmos., 4, 81-91.

Gunn, K.L.S., 1960: Snowfall rates at Montreal. Proc. 8th Wea. Radar Conf., 175-178.

Hervier, R., J. Squarise, R. Pejoux and G. Soulage, 1967: Un analyseur de pouvoir glacogene automatic. J. Rech. Atmos. No. 2, 65-77.

Hidy, G.M., and J.R. Brock, 1970: The Dynamics of Aerocolloidal Systems. Oxford, Pergamon Press, 379 pp.

Hobbs, P.V., 1969: Ice multiplication in clouds. J. Atmos. Sci., 26, 315-318.

Irani, R.R., and C.F. Callis, 1963: Particle Size: Measurement, Interpretation and Application. New York, John Wiley and Sons, 165 pp.

Isaac, G.A., 1968: Variations in Atmospheric Ice Nucleus Concentrations. M.Sc. Thesis, Dept. of Meteor., McGill University, Montreal.

-----, and R.H. Douglas, 1971: Frequency distributions of atmospheric ice nucleus concentrations. J. Rech. Atmos., 5, 1-4.

-----, and R.H. Douglas, 1972: Another "time lag" in the activation of atmospheric ice nuclei. J. Appl. Meteor., To be published.

Isono, K., and T. Tanaka, 1966: Sudden increase of ice nucleus concentration associated with thunderstorm. J. Met. Soc. Japan, Ser. II, 44, 255-259.

-----, M. Komabayasi, T. Takahashi, and T. Tanaka, 1966: A physical study of solid precipitation from convective clouds. Part II. J. Met. Soc. Japan, Ser. II, 44, 218-226.

Jiusto, J.E., 1968: Snow crystal development in supercooled clouds. Proc. 1st National Conf. Wea. Mod., 287-295.

-----, 1971: Crystal development and glaciation of a supercooled cloud. J. Rech. Atmos., 5, 69-85.

Junge, C.E., 1963: Air Chemistry and Radioactivity. London, Academic Press, 382 pp.

Langer, G., 1966: Further development of an acoustic particle counter. Paper presented to Contamination Control Meeting. Houston, Texas.

-----, 1969: Evaluation of NCAR ice and cloud condensation nucleus counters. Proc. 7th Intn'l. Conf. Condensation and Ice Nuclei. Vienna and Prague, 288-291.

-----, 1971: Comments regarding operation of the NCAR ice nucleus counter. J. Atmos. Sci., 28, 1074-1076.

-----, and J. Weickmann, 1971: Detailed evaluation of the NCAR ice nucleus counter--initial report. Intn'l. Conf. Wea. Mod., Canberra, 45-50.

-----, J. Rosinski, and C.P. Edwards, 1967: A continuous ice nucleus counter and its application to tracking in the atmosphere. J. Appl. Meteor., 6, 114-125.

Langleben, M.P., 1954: The terminal velocity of snowflakes. Quart. J. Roy. Meteor. Soc., 80, 174-181.

Marwitz, J.D., 1971: The Structure and Motion of Some Severe Hailstorms. Ph.D. Thesis, Dept. of Meteor., McGill University, Montreal.

Mason, B.J., 1968: The initiation of the ice phase in the atmosphere. Proc. Intn'l. Conf. Cloud Physics, Toronto, 162-173.

Mossop, S.C., 1970: Concentrations of ice crystals in clouds. Bull. Amer. Meteor. Soc., 51, 474-478.

Munn, R.E., 1970: Biometeorological Methods. London, Academic Press, 336 pp.

Nakaya, U., and T. Terada, 1934: Simultaneous observations of the mass, falling velocity and form of individual snow crystals. J. Fac. Sci. Hokkaido Univ., Ser. II, 1, 191.

Ragette, G., 1971: The low level mesoscale wind field of Alberta hailstorms. Sci. Rep. MW-69, Stormy Weather Research Group, McGill University, Montreal.

Rosinski, J., G. Langer, G.T. Nagamoto, T.C. Kerrigan, and F. Prodi, 1971: Natural ice-forming nuclei in severe convective storms. J. Atmos. Sci., 28, 391-401.

Ryan, B.F., and W.D. Scott, 1969: Ice nuclei and the onset of rainfall. J. Atmos. Sci., 26, 611-612.

Sax, R.I., and P. Goldsmith, 1972: Nucleation of water drops by Brownian contact with AgI and other aerosols. Quart. J. Roy. Meteor. Soc., 98, 60-72.

Scrase, F.J., 1935: The sampling errors of the Aitken nucleus counter. Quart. J. Roy. Meteor. Soc., 61, 367-379.

Siegel, S., 1956: Nonparametric Statistics. London, McGraw Hill, 312 pp.

Slinn, W.G.N., 1971: Time constants for cloud seeding and tracer experiments. J. Atmos. Sci., 28, 1509-1511.

-----, and J.M. Hales, 1970: Phoretic processes in scavenging. Precipitation Scavenging (1970), U.S. Atomic Energy Commission, CONF-700601.

Soulage, G., 1961: Origins, concentrations and meteorological importance of atmospheric ice nuclei. Nubila, 4, 43-67.

-----, 1965: Methods of measurement of ice nuclei concentrations. Pageoph., 60, 183-188.

Stansbury, E.J., and G. Vali, 1965: Experiments on the nucleation of ice 1961-63. Sci. Rep. MW-46, Stormy Weather Research Group, McGill University, Montreal.

Steele, R.L., and F.W. Smith, 1968: An experimental facility for simulation of adiabatic cloud processes. Proc. 1st Natn'l. Conf. Wea. Mod., Albany, 316-325.

-----, and C.I. Davis, 1969: Variations of ice nuclei effectiveness with liquid water. J. Atmos. Sci., 26, 329-330.

-----, C.P. Edwards, L.O. Grant, and G. Langer, 1967: A calibration of the NCAR Acoustical Ice Nucleus Counter. J. Appl. Meteor., 6, 1097-1107.

Squires, P., 1952: The growth of cloud drops by condensation. Aust. J Sci. Res., A, 5, 59-86.

Takeda, T., 1968: The effects of the time lag in the activation of atmospheric ice nuclei on the number of ice crystals in cloud. J. Met. Soc. Japan, 46, 69-75.

Vali, G., 1966: Sizes of atmospheric ice nuclei. Nature, 212, 384-385.

-----, 1968: Ice nucleation relevant to formation of hail. Sci. Rep. MW-58, Stormy Weather Research Report, McGill University, Montreal.

-----, 1971a: Quantitative evaluation of experimental results on the heterogeneous freezing nucleation of supercooled liquids. J. Atmos. Sci., 28, 402-409.

-----, 1971b: Freezing nucleus content of hail and rain in Alberta. J. Appl. Meteor., 10, 73-78.

Vittori, O.A., and V. Prodi, 1967: Scavenging of atmospheric particles by ice crystals. J. Atmos. Sci., 24, 533-538.

Warner, J., 1957: An instrument for the measurement of freezing nucleus concentration. Bull. Obs. Puy de Dome, 33-47.

-----, and T.D. Newnham, 1958: Time lag in ice crystal nucleation in the atmosphere, Part I Experimental. Bull. Obs. Puy de Dome, No. 1, 1-10.

Weiss, M., 1964: The Distribution of Rainfall with Rate. M.Sc. Thesis, Dept. of Meteor., McGill University, Montreal

Whytlaw-Gray, R.W., and H.S. Patterson, 1932: Smoke, London, E. Arnold and Co., 192 pp.

Woods, J.D., and B.J. Mason, 1964: Experimental determination of collection efficiencies for small water droplets in air. Quart. J. Roy. Meteor. Soc., 90, 373-381.

Zawadzki, I.I., and E. Ballantyne, 1970: HARPI: a new weather radar display. Quart. J. Roy. Meteor. Soc., 96, 144.

Zimmer, C.E., and R.I. Larsen, 1965: Calculating air quality and its control. J. Air Pollution Control Assoc., 15, 565-572.